



score

D3.4 - User document for the downscaling analysis tools and data

DATE OF DELIVERY - 30/12/2021

AUTHORS:

Carlo Brandini, Alberto Ortolani, Consorzio LaMMA & CNR

Francesca Caparrini, Andrea Cucco (CNR);

Stefano Taddei, Massimo Perna, Michele Bendoni (LAMMA);

Michele Baia (MBI);

Iulia Anton, Salem Gharbia (ATU Sligo).



This project has received funding from the European Union's Horizon 2020 research and innovation programme under grant agreement No 101003534



Project acronym	SCORE
Project title	Smart Control of the Climate Resilience in European Coastal Cities
Starting date	01.07.2021
Duration	48 months
Call identifier	H2020-LC-CLA-2020-2
Grant Agreement No	101003534

Deliverable Information	
Deliverable number	D3.4
Work package number	WP3 - Regional and Local Projections, Analyses, Modelling and Uncertainties
Deliverable title	User document for the downscaling analysis tools and data
Lead beneficiary	LAMMA & ATU
Author(s)	Carlo Brandini, Alberto Ortolani, (LAMMA; CNR); Francesca Caparrini, Andrea Cucco (CNR); Stefano Taddei, Massimo Perna, Michele Bendoni (LAMMA);Michele Baia (MBI); Iulia Anton, Salem Gharbia (ATU Sligo).
Due date	31/12/2022
Actual submission date	30/12/2022
Type of deliverable	Report
Dissemination level	Public

VERSION MANAGEMENT

Revision table			
Version	Name	Date	Description
V 0.1	Carlo Brandini, Alberto Ortolani, (LAMMA; CNR); Francesca Caparrini, Andrea Cucco (CNR);	12/12/2022	First draft





	Stefano Taddei, Massimo Perna, Michele Bendoni (LAMMA); Michele Baia (MBI);		
V 0.2	Roberta Paranunzio (CNR) Chiara Cocco (UCD) Jacek Barańczuk (UG) Cecil JW. Meulenberg (ZRS)	23/12/2022	Internal review
V 0.3	Carlo Brandini, Alberto Ortolani, Francesca Caparrini (LAMMA/CNR); Andrea Cucco (CNR IAS); Stefano Taddei, Massimo Perna, Michele Bendoni (LAMMA); Michele Baia (MBI); Iulia Anton, Salem Gharbia (ATU)	28/12/2022	Second draft after internal review
V 1.0	Iulia Anton, Salem Gharbia (ATU Sligo);	30/12/2022	Final review

All information in this document only reflects the author's view. The European Commission is not responsible for any use that may be made of the information it contains.

LIST OF ACRONYMS AND ABBREVIATIONS

Acronym / Abbreviation	Meaning / Full text
AI	Artificial Intelligence
CDF	Cumulative Distribution Function
CCLL	Coastal City Living Lab
CI	Critical Infrastructure
CORDEX	Coordinated Regional Downscaling Experiment
CNN	Convolutional Neural Network
DEM	Digital Elevation Model
DL	Deep Learning
DMP	Data Management Plan
DoW	Description of Work





DT	Digital Twin
DTM	Digital Terrain Model
EBA	Ecosystem-Based Approaches
ECMWF	European Centre For Medium-Range Weather Forecasts
EFAS	European Flood Awareness System
ESA	European Space Agency
EWSS	Early Warning Support System
GIS	Geographic Information System
GCM	Global Climate Model, sometimes General Circulation Model
GRU	Gated Recurrent Unit
ICT	Information and Communication Technology
IR	Implementing Rules
IT	Information Technology
JRC	Joint Research Centre
NBS	Nature Based Solutions
NCEP	National Center for Environmental Prediction
NN	Neural Network
PM	Probability Matching
RPO	Research Performing Organisation
RCM	Regional Climate Model
SLR	Sea Level Rise
WP	Work Packages





BACKGROUND: ABOUT THE SCORE PROJECT

The intensification of extreme weather events, coastal erosion and sea-level rise are significant challenges to be urgently addressed by European coastal cities. The science behind these disruptive phenomena is complex, and advancing climate resilience requires progress in data acquisition, forecasting, and understanding the potential risks and impacts of real-scenario interventions. The Ecosystem-Based Approach (EBA) supported by smart technologies has potential to increase climate resilience of European coastal cities; however, it is not yet adequately understood and coordinated at European level.

SCORE is a four-year EU-funded project aiming to increase climate resilience in European coastal cities. SCORE outlines a co-creation strategy, developed via a network of 10 coastal city 'living labs' (CCLs), to rapidly, equitably and sustainably enhance coastal city climate resilience through EBAs and sophisticated digital technologies.

The 10 coastal city living labs involved in the project are: Sligo and Dublin, Ireland; Barcelona/Vilanova i la Geltrú, Benidorm and Basque Country, Spain; Oeiras, Portugal; Massa (including the coastal area of Marina di Massa), Italy; Piran, Slovenia; Gdansk, Poland; Samsun, Turkey.

SCORE will establish an integrated coastal zone management framework for strengthening EBA and smart coastal city policies, creating European leadership in coastal city climate change adaptation in line with the Paris Agreement. It will provide innovative platforms to empower stakeholders' deployment of EBAs to increase climate resilience, business opportunities and financial sustainability of coastal cities.

The SCORE interdisciplinary team consists of 28 world-leading organisations from academia, local authorities, RPOs, and SMEs encompassing a wide range of skills including environmental science and policy, climate modelling, citizen and social science, data management, coastal management and engineering, security and technological aspects of smart sensing research.





EXECUTIVE SUMMARY

This document is a deliverable of the SCORE project, funded under the European Union's Horizon 2020 research and innovation programme under grant agreement No 101003534.

The D3.4, related to Task 3.2 and entitled "User document for the downscaling analysis tools and data ", is a WP3 deliverable, namely a report describing the downscaling procedures and models packaged contained in the deliverable D3.3, providing also what necessary for a proper use, and including a synthetic description of the datasets to be produced.

The aim of this deliverable, is to specify in detail the downscaling procedures used in the project, and developed within WP3, to provide local-scale data. Such data feed urban-scale models, enabling project critical activities such as flood risk analysis (WP6), the evaluation of the effectiveness of EBA solutions (WP7), the design of sensor networks for citizen-science activities (WP4), the development of a Digital Twin of coastal cities (WP8). The same data are going to be part of the project's data sharing platform (WP5).

LINKS WITH OTHER PROJECT ACTIVITIES

The activities of WP3 and in particular those of Task 3.2 are closely linked to all the other WPs of the project in a much more evident way than in the diagram in Fig. 1.

In practice, downscaling procedures are one of the main engines of data production in the project.

The local-scale climatological data, produced by this Task, are essential to enable the performance of several activities including those of WP3 itself, in this case with reference to statistical analysis (task 3.3), urban flooding models (task 3.4), coastal erosion models (task 3.5), and testing (task 3.6).

In addition, there are much more direct and obvious relationships with WP4, WP8, and WP7, which relate not only to the production of the data needed to perform these activities but, fundamentally, very necessary to define some methodological approaches of these WPs.





Figure 1. SCORE WPs interaction.





TABLE OF CONTENT

1. Introduction	10
1.1. Scope of this report	10
1.2. The meaning of downscaling	11
1.2.1. Dynamic downscaling	12
1.2.2. Statistical and stochastic downscaling	13
1.2.3. Methodology to downscale climate information	14
1.2.4. Downscaling to enable the simulation of urban-scale scenarios	16
1.3. Climate simulation models for coastal cities	16
2. Statistical downscaling of atmospheric fields	19
2.1. Objective	19
2.2. Introduction to the method	20
2.3. The neural network downscaling process	23
2.4. Mapping the surrogate dataset to the projection dataset	26
2.5. The local downscaling process	28
3. Downscaling of sea levels	30
3.1. Model description	30
3.2. Model implementation	32
3.2.1. Numerical mesh	33
3.2.2. Atmospheric forcing and ocean data	34
3.2.3. Model and simulation setup	35
3.3. Output data description	35
4. Downscaling of waves	37
4.1. Model description	37
4.2. Model implementation	39
4.2.1. Numerical mesh	39
4.2.2. Atmospheric forcing	41
4.2.3. Model and simulation setup	41
4.3. Output data description	42
5. Hydrological downscaling	45
5.1. Hydrological models as a downscaling tool	45





5.2. LISFLOOD model	45
5.2.1. Model overview	46
5.2.2. Model implementation	48
5.2.3. Settings file	49
5.2.4. Input datasets	50
Meteorological forcing	50
Static maps	50
Topography	51
Land Use maps	51
Land Use depending maps	51
Soil hydraulic properties	53
Channel geometry	53
Leaf area index	54
Other data	54
5.2.5. Outputs	55
6. Conclusions and recommendation	56
7. References	58





1. INTRODUCTION

1.1. Scope of this report

This report D3.4 "User document for the downscaling analysis tools", as the result of Task 3.2 "Downscaling analysis tools", is strictly related to the other deliverable D3.3 "Package of downscaling analysis tools", of which it is not only a descriptive part, but of which it is also a technical-scientific one.

The report describes the tools through which local-scale climate data are produced starting from: 1) climate data provided by global and regional scale climate models; 2) geographical knowledge of the territory through the combination of local specificities (orography, coastline, land use, etc.) and the collected observational data.

In practice, the concept of downscaling that we use in SCORE is not only to produce local scale data that may be of interest in their own right, but also to enable the creation of new downstream models (urban scale models) that are crucial, for example, for flood mapping and the study of adaptation solutions.

As far as the links with the other WPs of the project are concerned, these became even more important than initially foreseen in the DoW document.

Work Package	Interactions
WP1	Knowledge on past extreme climate data is essential to compare with the climate change scenarios produced by this Task, as well as to validate dynamic models by using them to reproduce past situations
WP2	The interest in the data produced by this Task is central to the activities of the CCLLs
WP3	The data produced by the tools in this Task enable other downstream services/models, and in particular the hydraulic and land-sea interaction models used for urban-scale flooding (Task 3.4) and also the long-term coastal evolution models (Task 3.5)
WP4	The design of the low-cost sensor network and citizen science activities are strongly connected with the need to improve the spatial representativeness of the data, and therefore WP3 and WP4 are naturally complementary
WP5	The data produced by WP3 and from this Task in particular, especially the time series of climate projection data, are among the main sources of data production for the entire project
WP6	Data produced by WP3 are fundamental for risk estimations
WP7	Data produced by WP3 are needed to design NBS and select EBAs





WP8	Data produced by WP3 are a fundamental component to drive the models used by the DT
WP9	WP3 models and models defined in Task WP3.2 must be disseminated not only to a scientific audience, but as well transferred to the various contexts also through specific training activities which involve non-scientists

In this report we will attempt to describe the characteristics of the models used for the creation of a time series of data necessary for the implementation of project activities in coastal cities.

Coastal cities have specificities compared to the surrounding natural coastal territory: being located on the sea, they are the parts of the territory perhaps in which humans residents are most susceptible to the effects of climate change, also due to the effects of Sea Level Rise (SLR).

This requires that the data of greatest interest include marine data, alongside traditional meteorological and hydrological data, as they are needed to estimate, for example, the effects of storm surges, extreme sea levels, or coastal erosion.

The data covered by this report are therefore:

- wave data, used for various applications, such as estimating run-up extremes or calculating coastal morphodynamics;
- sea level data, used for estimating storm surge effects and interactions with urban hydraulics;
- hydrological data such as flow rates and levels, that are needed for urban flooding models but also to improve understanding on the effects of EBAs solutions;
- meteorological data, needed to force other models, for example, to give a more correct distribution of the rainfall input to hydrological models.

Each of these datasets requires to be produced with tools, mainly models, different from each other. In the following, we will describe them, keeping in mind the relevance of the present task within the project.

1.2. The meaning of downscaling

A common need for all project components is to have data available at the local scale, namely the urban scale, to assess the long-term consequences of climate change on coastal cities. The source data, described in deliverables D3.1 and D3.2 of the WP3, Task 3.1, component of the project, are climate models, either at a global or regional scale.

There is a large gap between the data that are produced from Global Climate Models (GCM), with a resolution that can be on the order of 0.5° or 0.25° i.e. on the order of 25-50 km at mid-latitudes, or -when available- from regional climate models (RCM), with a resolution that typically goes as low as 0.125-0.1° i.e. on the





order of 10-12 km at mid-latitudes, and the need for local (urban) scale data for the various needs (on the order of hundreds or tens of meters).

Downscaling means taking information at large scales to infer effects at local scales. Thus, to take for example weather forecasting: a common practice is to use data from a global forecasting model (such as those produced by forecasting centres such as ECMWF or NCEP), to make forecasts at the regional and/or local scale. Thus, with reference to climate projections, downscaling of climate models is an attempt to bridge the gap between global and local effects through techniques or models that take into account local specificities, and that are able to simulate locally the effects induced by the processes predicted by large-scale climate models. In general, climate information from global or regional climate models has a low resolution, for which an entire region can be represented by only a few grid cells. Each cell represents a single value, which may be representative of an area that, for example, is 100-150 km² (in the case of a regional model with 10-12 km² resolution). A key issue why downscaling is necessary, is that global climate models do not adequately account for variations in vegetation, complex topography and coastlines, which all are important aspects of the physical response governing the regional/local climate change signal.

The modeling of the effect of a changing climate at local scale examines relatively small areas down to a few square kilometres in detail, that is at a much higher resolution than generally offered by global climate model simulations. Such information supports analyses regarding the impact of climate change, and the assessment and planning of adaptation strategies that are vital in many vulnerable regions of the world, which, undoubtedly, include coastal cities.

Normally, there are two general strategies for downscaling:

- dynamic downscaling uses sub-regional scale models with high spatial resolution (on the order of a few km) over a limited area, and is fed by the large-scale conditions of a GCM or RCM.
- statistical downscaling is the method by which statistical relationships are derived between observed small-scale variables (often at the weather station level) and larger-scale variables (GCM or RCM). The predicted values of large-scale variables obtained from GCM projections of future climate are then used to drive statistical relationships and thus estimate small-scale details of the future climate.

Both methods have advantages and disadvantages.

1.2.1. Dynamic downscaling

Dynamical downscaling is based on numerical models that solve a set of discretized equations which reproduce a set of mathematical equations describing the temporal evolution of the phenomena under investigation. For example, in the case of atmospheric or marine circulation, models solve the primitive equations of motion that represent the temporal evolution of fundamental variables such as velocity, temperature, pressure, density, etc. Dynamic downscaling has the great advantage of providing data in a way that can be considered physically consistent. This means that the equations governing the evolution of the atmosphere or the sea, are solved in a finer grid in which the representation of certain physical features (e.g., details of orography, land use, coastline, etc.) is much more detailed than in the parent model. For the sake





of clarity, it is important to specify that on the basis of the scale of the main modelled processes, different simplifications/approximations can be applied to the governing equations.

The large-scale model data are used, normally, as initial conditions and boundary conditions for local-scale models. The large-scale variables used as initial and boundary conditions are normally interpolated onto the higher-resolution grid, and the model "fits" the solution of the equations into the new domain, after a certain period required to activate the finer-scale dynamics.

This adaptation period (often referred to as spin-up) varies greatly from model to model. Models that quickly lose memory of initial conditions are, for example, atmospheric models, where the spin-up time is usually short (6-12 h). Wave prediction models have similarly small spin-up times.

In contrast, models in which it is necessary to extend the spin-up time are, for example, marine circulation models describing baroclinic processes and thermohaline effects, in which several dynamics only come into effect after many time steps. In general, few days are required to completely activate surface dynamics, while deep circulation dynamics, related to the distribution of water masses within the oceans, need very long times, even on the order of several years.

Hydrological models, to simulate processes related to infiltration and sub-surface runoff, also require long timescales.

The main disadvantage of dynamic downscaling is the computational cost. The finer the grid, the larger the computational cost, due to constraints related to the integration time step (e.g., stability conditions). This condition means that computation at very fine resolutions and over very large areas is impractical even for the best performing computational machines.

Another aspect to consider is that the resolution ratio between the "parent" model and the "child" model should never be too high. Many dynamic models typically use a ratio of 1:3 or 1:5, seldom higher, which is not recommended in any case. This constraint significantly affects the dynamic downscaling methodology if the goal is, for example, to provide local-scale data, where the required local-scale resolutions are very high.

Assume that we intend, for example, to get climate data at an urban-scale resolution of a few tens of meters (e.g., 100 m). Moving from a RCM, which has a resolution of the order of 12 km, to such very high resolution would require at least 3 consecutive models nested into each other, e.g., maintaining a 1:5 ratio of parent model resolution to child model resolution (from 12 km to 2.5 km; from 2.5 km to 500 m; from 500 m to 100 m), which is very challenging because each model is simultaneously "child" of a less resolved model and "parent" of a more "resolved" model. This telescoping approach to nesting is not practical for most uses.

To overcome this complication, the use of unstructured mesh numerical methods is normally very effective, because it allows for high resolution only where it is strictly necessary (in our case, near coastal cities, or at any specific area of interest), while also simplifying procedurally the implementation of downscaling.

1.2.2. Statistical and stochastic downscaling

Statistical and stochastic downscaling methods have very often been proposed to avoid the complications associated with the use of dynamic models. In the first case, a statistical link is established between large-scale variables (called predictors) and those that one wishes to describe at a local scale (called predictands),





in order to produce high-resolution realisations of the latter. Essential for statistical downscaling is the availability of local observations (i.e. meteorological, hydrological, marine data). The results of statistical downscaling improve with higher quality and duration of the observed historical data. Having good data for a particular weather or marine station, enables to downscale the climate model for that particular observing point. At the same time, having a good gridded data set locally available (i.e. from a hindcast model), does permit downscaling on that grid. Then, for statistical downscaling, a statistical relationship is developed between the observed historical climate data and the climate model output for the same historical period. This relationship is used to develop future climate data.

Stochastic downscaling methods, although they can reproduce time series of data at a given point, cannot be considered as substitutes for physically-based regional models (i.e., dynamic downscaling). Instead, they are a way to introduce variability in precipitation fields at scales not resolved in global or regional models.

Among the statistical/stochastic methods, the application of Artificial Intelligence (AI) methods for downscaling has become more and more important. In particular, a new generation of AI methods are gaining more attention due to better training compared to older generations, including Deep Learning (DL) and Convolutional Neural Network (CNN) methods.

1.2.3. Methodology to downscale climate information

The downscaling procedure can be applied to different typologies of datasets. Indeed, it is possible to downscale operational forecast data, reanalysis and climate information (Benestad, 2016).

Concerning the downscaling of climate scenarios (or projections, IPCC, 2013), it is important to evaluate how much we can trust the results from the RCM model that downscaled the GCM that produced the particular scenario.

Hindcast simulations take initial and boundary conditions from a reanalysis. The reanalysis is produced by a data assimilation system which ingests many kinds of observations that are representative of the true atmospheric state. As a consequence, the RCM maintains the temporal correlation with what is observed in nature (e.g., extreme events).

In case initial and boundary conditions are taken by a GCM without data assimilation we are considering a historical simulation. This kind of simulation is used to have information about the interaction between GCM and RCM, but the synchronization with the observed climate is lost. However, the importance lies in the fact that the boundary conditions for the downscaling of climate scenarios can be taken from the same GCM.

For the purposes of the project we need to downscale the wave climate, the sea level, and the rainfall rate. The simulation of these variables requires the data provided by a RCM. More specifically, for the adopted approach the following variables are needed:

- for waves, surface wind speed for U (eastward direction) and V (northward direction) components (uas , vas);
- for sea level, surface wind speed for U and V components (uas , vas), mean sea level pressure (psl);
- for rainfall rate, precipitation (pr).





Rainfall rate is then used in the hydrological model, applied to a specific river basin, to determine the flow rate at a closure section of the river.

A sketch of the modelling chain is reported in Figure 1.1.

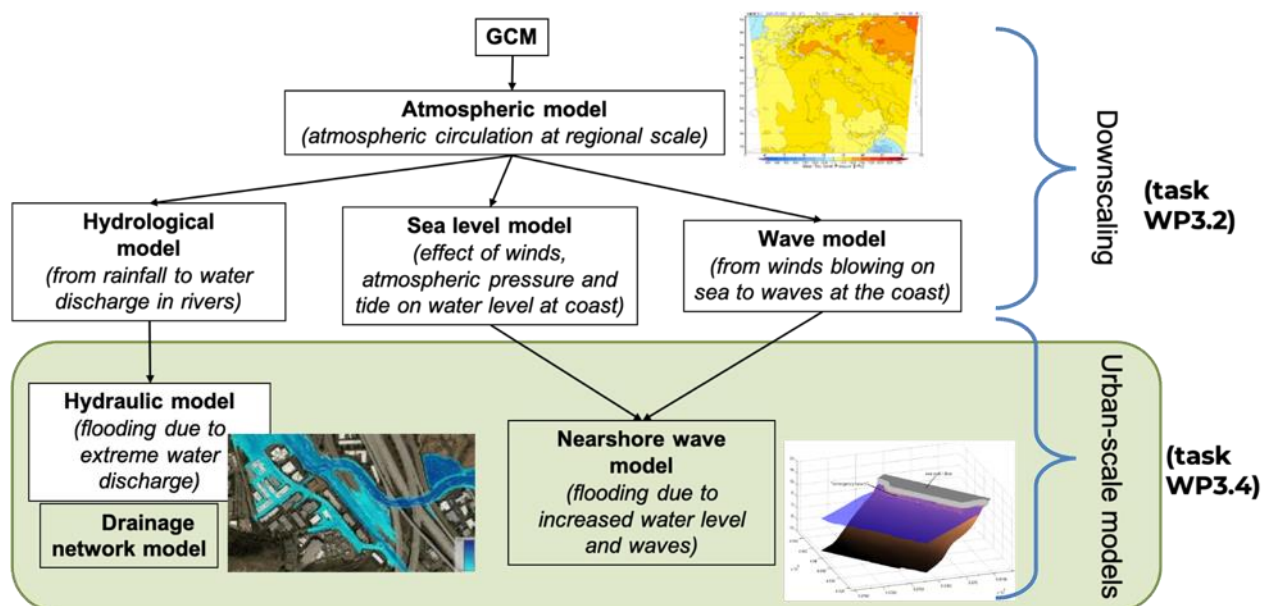


Figure 1.1. Sketch of the modelling chain employed to downscale climate data up to the urban scale.

In our case, we opted for the ALADIN 63 RCM (Coppola et al., 2021; Vautard et al., 2021) employed in the EUROCORDEX project (Jacob et al., 2014), which is the European branch of the CORDEX project and is aimed at the production of downscaled simulation of GCM from the Coupled Model Intercomparison Project Phase 5 (CMIP5, Taylor et al., 2012). The reason for this choice was principally due to the availability of the physical variables needed to simulate wave properties, sea water level and rainfall rate, at a sufficiently temporal frequency, that is 3 hours. Also because ALADIN 63 is the same RCM used to produce historical (1950-2005), evaluation (1979-2019) and scenario (2006-2100) runs.

Furthermore, the RCMs related to the EUROCORDEX project are run on a geographical domain containing all the CCLLs of the project (Figure 1.2).

Our strategy to downscale climate data is indeed to simulate, wave properties, water levels and rainfall rates:

- an evaluation run to validate the models employed for the downscaling, by comparing modelled results to observations;
- a historical run to be compared to the evaluation run from a statistical point of view. Since we are particularly interested in extreme events, we evaluate the degree of similarity between the extreme value distribution from the evaluation and historical run, computed for the same reference period;
- two runs associated with the RCP4.5 and RCP8.5 scenarios.

The evaluation run is based on the modelling chain ERA-INTERIM (Dee et al., 2011), ALADIN 63. Whereas the historical and scenario runs are based on the modelling chain CNRM-CM5 (Voldoire et al., 2013), ALADIN 63. The resolution of the ALADIN 63 model is 0.11° (roughly 10 km at mid latitudes).





Figure 1.2. Extension of the EUROCORDEX domain.

1.2.4. Downscaling to enable the simulation of urban-scale scenarios

Within the project, a thorough discussion took place to decide which methods should be applied to downscale climate fields.

The discussion took place at two levels:

- 1) a first level can be defined as user-oriented, i.e. it relates to the use of the data for specific applications;
- 2) a second level concerns the analysis of methods in relation to the need to produce data according to specifications that are sufficiently state-of-the-art, but at the same time sustainable with regard to their concrete application within the project timeframe and the available human and computing resources.

Figure 1.1 clarifies the approach used in SCORE for downscaling. Rather than being concerned only with having more resolved physical fields for certain variables of interest, the goal is to enable a series of detailed models, at local and urban scales, to describe flooding phenomena, as well as possible risk reduction and adaptation strategies.

Another need is to have local-scale data available for the simulation of long-term dynamics, such as coastal erosion/progradation. The availability of atmospheric data downscaled at regional scale from various initiatives, such as EUROCORDEX and MEDCORDEX, allows us to directly use them as atmospheric forcing for the above-mentioned models. This availability of data from regional-scale models was considered sufficient to describe, albeit in an approximate manner, even in light of recent scientific literature in the field, the atmospheric forcing that drives wave and sea level modelling.

1.3. Climate simulation models for coastal cities

In climate projections, whether on a global, regional or local scale, models certainly play the most important role. However, it is also important to have observations, so as to have a dataset of observed data that is representative of both temporal variability and long-term trends, and preferably distributed over several points in the territory, representative of different exposures, orographic conditions, etc. The role of the





observations in the models is: 1) to validate and calibrate the calculation models at least as far as the historical part is concerned; 2) to train artificial intelligence algorithms; 3) to estimate model-internal parameters, which may also be carried out by means of assimilation techniques (e.g. Kalman filtering).

The choice of models to be used for the project focused mainly on open source models, possibly community models, because the development of these models goes on over the years and transparently incorporates all the updating efforts made by a large scientific community. Secondly, it is important that at the level of individual coastal communities these models can be disseminated and used by local users, technicians and scientists, with a non-exaggeratedly specialised background, also transferred through specific training activities and can be used without additional costs.

In terms of modelling choices, another general preference was given to models that provide greater flexibility of use by avoiding the use of nesting techniques. In particular, especially for marine models, the adoption of unstructured mesh models was preferred. This is because the aim of the project is not to build climate services on uniform grids, or with a uniform level of output, but to focus on specific coastal areas, in order to build tools that guarantee the provision of highly detailed data for those areas and -possibly- maintain a certain easiness to replicate/adapt procedures and exportability of the methods adopted to other contexts.

The ten Coastal City Living Labs that are part of the SCORE project have different capacities and skills in reference to climate modelling.

CCLLs that have been chosen as frontrunners for WP3 are:

- Massa (Italy)
- Province of Barcelona (Spain)
- Oarsoaldea (Spain)
- Alicante (Spain)
- Samsun (Turkey)

The implementation of downscaling models in coastal cities can be accompanied by some problems that will become clear later.

For marine models, problems concerning physics of wave formation and propagation or sea level changes require defining the model over areas normally large enough to collect all possible contributions from energy or mass propagation over long distances (normally this distance is referred to as fetch). For coastal cities placed in semi-enclosed seas such as the Mediterranean, the Black Sea, the Baltic Sea, this does not pose particular problems, but does require some care in defining the computational model.

Conversely, for cities facing the Atlantic Ocean, this approach requires much greater attention in identifying possible contributions related to wave energy and storm surge formation at a given point.

Hydrologic modelling also has issues that need to be properly addressed. Indeed, there is great variability in the size of the hydrologic basins and their characteristics. While for very large basins the representation of rainfall and atmospheric variables from GCMs or RCMs can be considered adequate, the same cannot be said for smaller basins that would require a much finer representation of rainfall. Dynamic downscaling of the





atmospheric component is not carried out by the project, due mainly to limitations of budget and timing. However, a procedure based on AI algorithms is described to achieve local-scale downscaling of rainfall data. As for the CCLLs followers, only the wave and sea level related components will be simulated by the core team, but support, assistance and technical training how to effectively make use of the methodologies described in this report, is planned.





2. STATISTICAL DOWNSCALING OF ATMOSPHERIC FIELDS

2.1. Objective

As we know from the SCORE D3.1 and D3.2, a number of datasets exist for atmospheric projections up to the year 2100, that are available over the SCORE target geographical domain, i.e. the Euro-Mediterranean area, physically downscaled from global projections and providing horizontal (i.e. ground) spatial resolution up to about 12 km and temporal intervals up to 3h. It is worth to note that the spatial resolution is the real one unit set, once the model is physically run. While the temporal interval is depending on the averaged and stored outputs, with the run time-steps always much shorter than this (roughly more than two order of magnitudes shorter).

A 3h temporal resolution can be generally considered acceptable for the hydrological modelling of the SCORE coastal city basins, according to their response time to the precipitation events. Maybe, for a few smaller basins, with a faster response time, a 1h resolution could make some non-negligible differences on hydrological modelling and consequently on hydrological projections, which in SCORE is the main application of the precipitation projections and of the other atmospheric parameter ones. Anyway we assume this to be not critical for hydrological projections and we adopt 3h temporal resolution as suitable for any SCORE basins, thus not setting up any temporal downscaling strategy.

For what concerns the horizontal spatial resolution, 12 km can be instead critical for a number of SCORE hydrological basins, being their dimension as large as few model ground pixels. This can mean that some model pixels can belong only partially to the basin and that they can average on sub pixel orographic and maybe precipitation inhomogeneities, introducing non-negligible systematic errors on hydrological projections. In addition running a model at 12 km horizontal resolution means that any phenomenon happening at a smaller scale cannot be physically represented. This for instance typically happens with convective precipitation, that in some cases is not negligible or more often even dominant, so that it is necessary to model it through statistical empirical schemes, that use some model atmospheric features (at the available coarse resolution) to infer how much convective precipitation should be generated within any model ground pixels. This is a non-trivial way to account for non-negligible sub-pixel (i.e. model sub-grid) phenomena, that anyway can bring relevant errors. This typically happens in operational forecasts, and motivates the effort of running higher resolution models, nested in lower resolution ones, from global models to regional ones. Focusing on precipitation, the final objective is to be more reliable in precipitation intensity forecasts, increasing also the precision on where and when it will happen. When dealing with projections, if you think about precipitations (but this similarly holds for other parameters), the scheme approximations and related errors propagate also in the statistical distributions, so that the result of downscaling should be to improve the phenomena description in order to have more reliable statistics. In addition we would have





statistical information on smaller pixels, improving the geographical details for the benefit of the hydrological modelling.

Similarly to the aforementioned operational approach, spatial downscaling could be achieved “simply” nesting a state of the art atmospheric model into the available better projection data, and running such a model chain for the whole projection range. Theoretically this is the more correct approach, but it can be very time consuming and computing demanding. In addition, there are a number of issues that have to be carefully addressed and verified to assure that the new projections are reliable and coherent with the coarser model they start from, including the need to care about the proper evolution of the greenhouse gases from the reference to the nested models. In sum, several aforementioned approaches are outside the SCORE project objectives and constraints, as clearly stated also in the project proposal.

In order to cope with the spatial resolution problem, especially thinking to the basins where it can be more critical, we have then designed a statistical approach for the downscaling, that makes use of a Neural Network (NN) approach, aimed at connecting coarse resolution projections to higher resolution grid data, according to a climatological dataset available at the target (i.e. higher) resolution. This approach has the non-secondary benefit to be similarly applied to generate also local downscaling, i.e. to produce scenarios of local measurements in a given point, according to a climatological dataset of in situ measurements. In the SCORE framework it means that we can generate projections of in-situ measurements in the coastal cities, applicable for instance to urban hydraulic modelling for digital twin applications.

2.2. Introduction to the method

In order to downscale a projection dataset with a statistical approach, it is mandatory to own a reference dataset for the study domain at the target spatial resolution (i.e., the one we want at the end of the process). It is necessary that both (the projection and the reference) datasets have a subset belonging to a temporal range exhibiting the same climatological features. It is also necessary that both subsets extend for a climatologically significant period. However, it is neither necessary that these two subsets refer to the same temporal range nor that they share any temporal overlapping.

In our test case, the projection dataset has been the Med-CORDEX (Ruti et al., 2022), a regional model centred in the Mediterranean basin. Depending on the forcing present in the model, we can divide the dataset in historical run (no forcing), evaluation run (measurement forcing) and projection runs (radiative forcing according to given development scenarios).

The subset exploited for tuning the downscaling process is from the historical mode, i.e. the model freely run but for the past (commonly used to verify the consistency between the reproduced statistics and the real atmosphere). Normally projections are available for different emission forcing scenarios, according to possible future (unknown) development scenarios associated to greenhouse gases concentration etc., while the historical subset is only one, according to the past (known) atmospheric and other environmental features. Note that in some datasets (including the one we used) we can find data referring to a number of past years, but run and archived as projections (this of course happens always but not only for data generated in projects concluded several years ago). In this case, we will consider, use and also refer to such data (in the atmospheric downscaling part of this document) as belonging to the historical mode, even if nominally





archived in the projection part of the dataset (paying attention to the adopted radiative forcing, that has to be close to what we know it really was).

Concerning these historical data, only the statistics between the model and the real atmosphere can be compared for consistency, not single phenomena, in fact such historical mode is never synchronised with Nature, e.g. through some direct or indirect assimilation process of real measurements. It means that, differently from models run for operational forecasts, the historical mode (exactly as the projection mode) does not simulate different phenomena in the right place at the right time, but, after a long enough period, it generates a set of statistics for phenomena consistent with the real one.

For the same past period, there is also a so called evaluation mode, which, differently from the historical one, is continuously forced by reanalyses products (that include observations from global measurement networks), thus forced to be synchronised to Nature as much as possible (useful to evaluate for instance the consistency of the model physics). This mode is not used in our spatial downscaling, because we expect a greater similarity in the behaviour between the historical-projection couple with respect to the evaluation-projection one, due to the presence of the forcing process in the evaluation mode, that has no counterpart in the projection phase. Anyway, we will see later that the evaluation mode turns out to be very useful for the local projections as defined in the previous paragraph.

It is worth to note that several other projection datasets have analogous historical and evaluation modes, so that the same repeated approach we are going to use and explain is applicable to the most advanced climatological projection datasets.

For what concerns the reference dataset, we have used a dataset generated by a 29-years run of the Moloch model (Capecchi et al., 2022) run at 2.5 km of horizontal spatial resolution over a domain as large as the Italian peninsula. Such a run has been continuously forced with ERA5 reanalyses data, implemented through a nested domain configuration based on limited-area numerical weather models (BOLAM/MOLOCH). The study region is situated in the North-Western Mediterranean Sea, in particular centred in Massa, Italy, and spanning between $8^{\circ}69'72''\text{E}$ – $11^{\circ}43'06''\text{E}$ and $43^{\circ}52'49''\text{N}$ – $44^{\circ}98'15''\text{N}$. In our activity we considered a subset of the last 12 years.

The projection dataset, or more precisely its historical mode subset, and the reference one are not directly comparable, because of their different resolution, and moreover due to the lacking of any synchronisation. From the reference dataset we have then generated a “surrogate dataset” with the same resolution of the projection dataset, with an upscaling procedure, applying a simple averaging process. Obviously the surrogate dataset results perfectly synchronised with the reference dataset and available for the same temporal and spatial domains. At the same time we expect that the surrogate dataset and the projection historical-mode subset should be statistically comparable, apart from some differences given by the differences in the two models, including the fact that the surrogate dataset was generated by a higher resolution model, capable to explicitly simulate smaller scale phenomena with respect to the projection one. Now we have two datasets, the reference and the surrogate ones, perfectly synchronised and overlapping, but at different spatial resolution, so perfectly usable to train a Neural Network (NN) procedure for downscaling from the surrogate resolution (equal to the projection one) to the reference resolution. Then we have identified two other datasets, the surrogate and the projection historical-mode subset ones, at the same resolution and available for a period of constant climatology (as assumed at the beginning), that are





expected to have comparable statistics, but with some foreseen differences that have to be matched by means of some proper transformation procedure. Figure 2.1 shows the synthesis of the downscaling method.

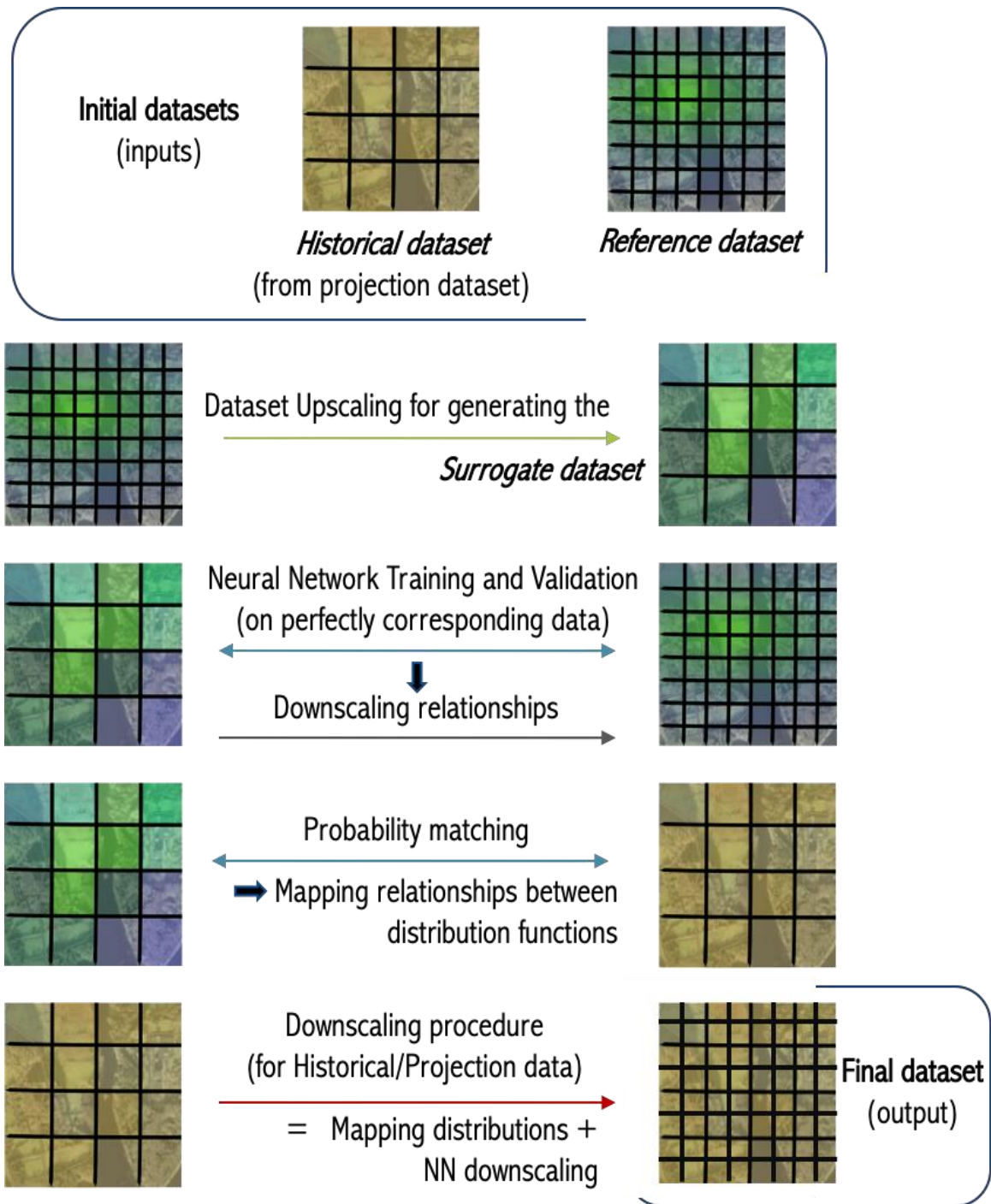


Figure 2.1. Synthesis of the statistical downscaling steps. From top to bottom: generation of a surrogate dataset from the upscaling of a high resolution dataset (climatologically significant); building a specific downscaling NN (more complex step) and training it to match the two perfectly corresponding reference-surrogate datasets; match surrogate and projection (historical mode) datasets having the same resolution; apply the whole downscaling process (map values from mapped distributions, then use the NN relationships) to the projection dataset (for the future scenarios).





2.3. The Neural Network downscaling process

Statistical downscaling uses large-scale information (predictor) to build relationships to a local weather variable (predictand). There are many statistical approaches that can be used to bridge the gap between the scale needed for a local prediction and the regional scale, for example reconstructing the time series of the variable at low scale (regression methods) or generating possible event in function of weather type index (weather type approaches) or using stochastic generator, like random Markov chain (stochastic weather generators). Choosing between one method or another depends strictly on the nature and the quantity of the data in the dataset available. The nature of the dataset and the temporal short range of our time series, for example, makes it impossible to use weather type or stochastic weather generators. Thus, in this work we consider the first approach and train a NN to find a relationship between the two different spatial scales.

The NN, more specifically in our case a CNN, has to find a local relationship between the predictor and the predictand directly from the data. The input is a tensor containing information about the predictor value in a pixel, eventually its neighbours and also spatial information - like orography and land cover (Copernicus Land Monitoring Service, 2018) – associated to the surrogate dataset. From these data the NN should predict the value of the high-resolution pixels in the reference data that are geographically close to the centre of each low-resolution pixel of the surrogate data. Considering the spatio-temporal correlation that exists between the atmospheric variables, we built a NN with layers that can properly capture the spatial and also temporal dependencies.

The architecture that have been adopted (see Figure 2.2 label and Table 2.1 for technical details) can be summarized as:

- a Convolutional layer (Conv2d), to capture the spatial relationship between the nearest pixels and to map a large-scale latent space;
- a layer with recurrent gate (GRU), to catch some temporal dependencies and temporal patterns in the large-scale latent space, processing temporally closest data (here three time steps);
- a fully connected layer (LinL), to map the spatio-temporal representation of the large scale predictor in the small scale predicted variable;
- a last layer (MeanL), that generates the final data at the reference resolution from the LinL output.

From the surrogate data we create a collection of surrogate images with dimension m - stacking the surrogate predictors and the spatial information of the surrogate data (latitude and longitude) - and temporal window w . For every pixel of the surrogate data, the NN reconstructs n pixels of the resolution of the reference data. In the reconstruction of the complete image of the reference data, we can have some overlapping, because two or more pixels of the surrogate data predict the same pixel of the reference data. In such cases the final image can be generated re-averaging the overlaps. In order to force the NN to predict the same values at the same pixel starting from different pixels of the surrogate data, we include the generation of the image in the learning process: namely we generate the downscaled image with a weighted average, where the weights are stored in the MeanL and learned in the training phase. The optimization of the NN is done with a L^2 loss (squared error loss, i.e. squared difference between a prediction and the actual value) over the values of the pixels of the image generated by the prediction of the net and corresponding values of the true image of the reference dataset.





The NN learning process was achieved using 9 years of data as training set (from 2008 to 2016 included), while the last available 3 years (2017, 2018 and 2019) were used as test set, i.e. to quantify the learning precision over data that the NN had never seen before. In Figure 2.3 some examples of output for different atmospheric variables are shown, where predicted means downscaled by the NN-based process.

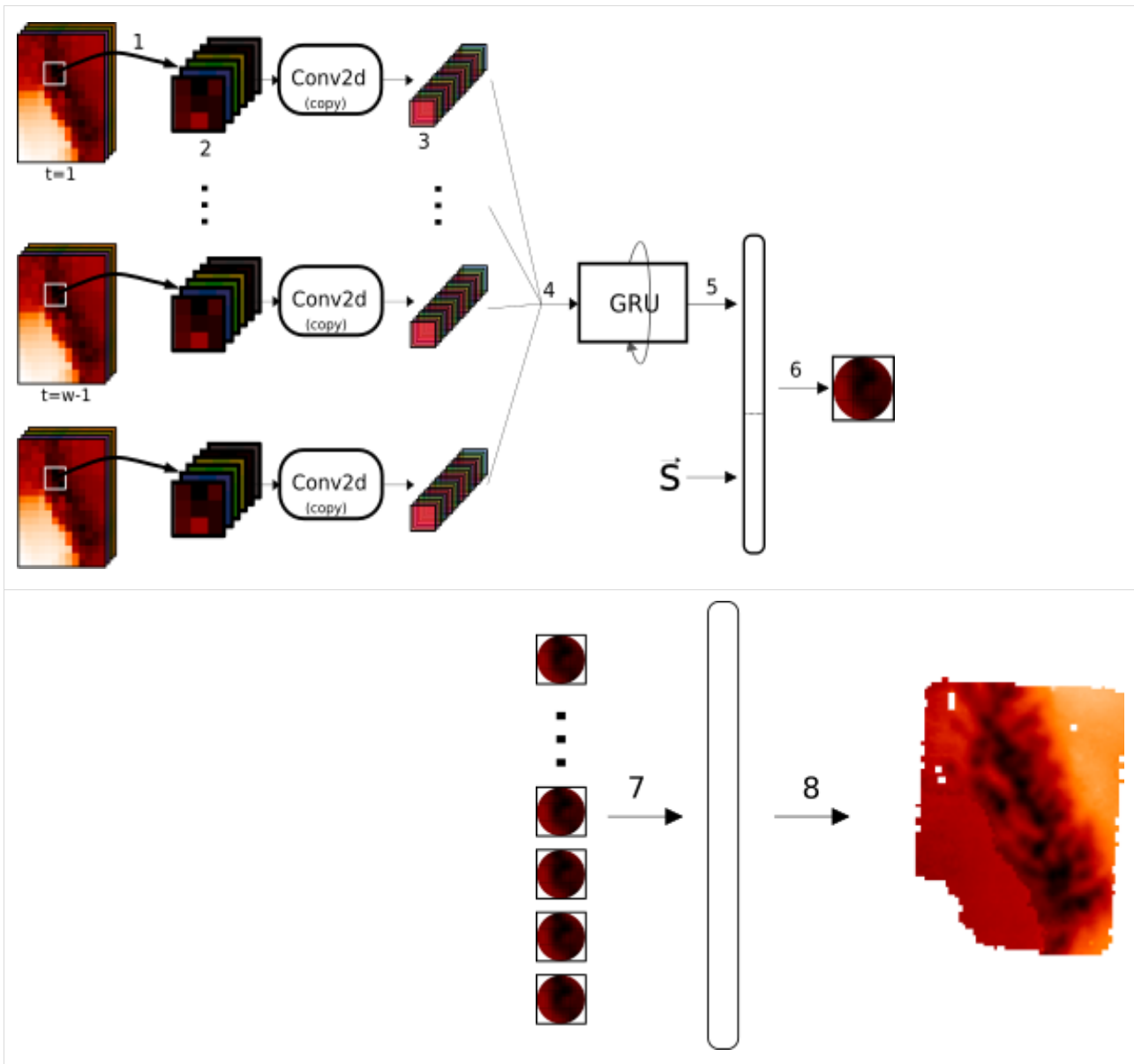


Figure 2.2. Top panel: for every time ($t, \dots, t=w$), we extract from the surrogate images (1) any single pixel with its nearest neighbours to create the input of the Conv2d layer (2), a tensor of size: $(m, 3, 3)$. As output (3) we obtain a vector of size: $(C_{out}, 1, 1)$, where C_{out} represents the number of channel outputs of Conv2d. We stack together this output (4) to obtain the GRU input, with size $(C_{out}, w, 1)$, that gives us the hidden representation (5) of the variables in surrogate pixels. The estimation of the value at the small scale (6) is done combining this hidden state with a State vector (S) that contains the spatial information of the reference data with the last LinL layer. This layer gives as output a vector that can be thought as the neighbours of the surrogate pixel. Bottom panel: for reconstructing the final image (8), we repeat the the top panel procedure for all pixels, then we combine the outputs (7) using the weights stored in MeanL.





	m	n	<u>Cout</u>	<u>size</u> GRU	<u>Size</u> <u>LinL</u>
<u>value</u>	#p + 2	100	32	64	100

Table 2.1. Hyperparameter of the NN used in the examples showed below. #p indicates the number of predictors chosen.

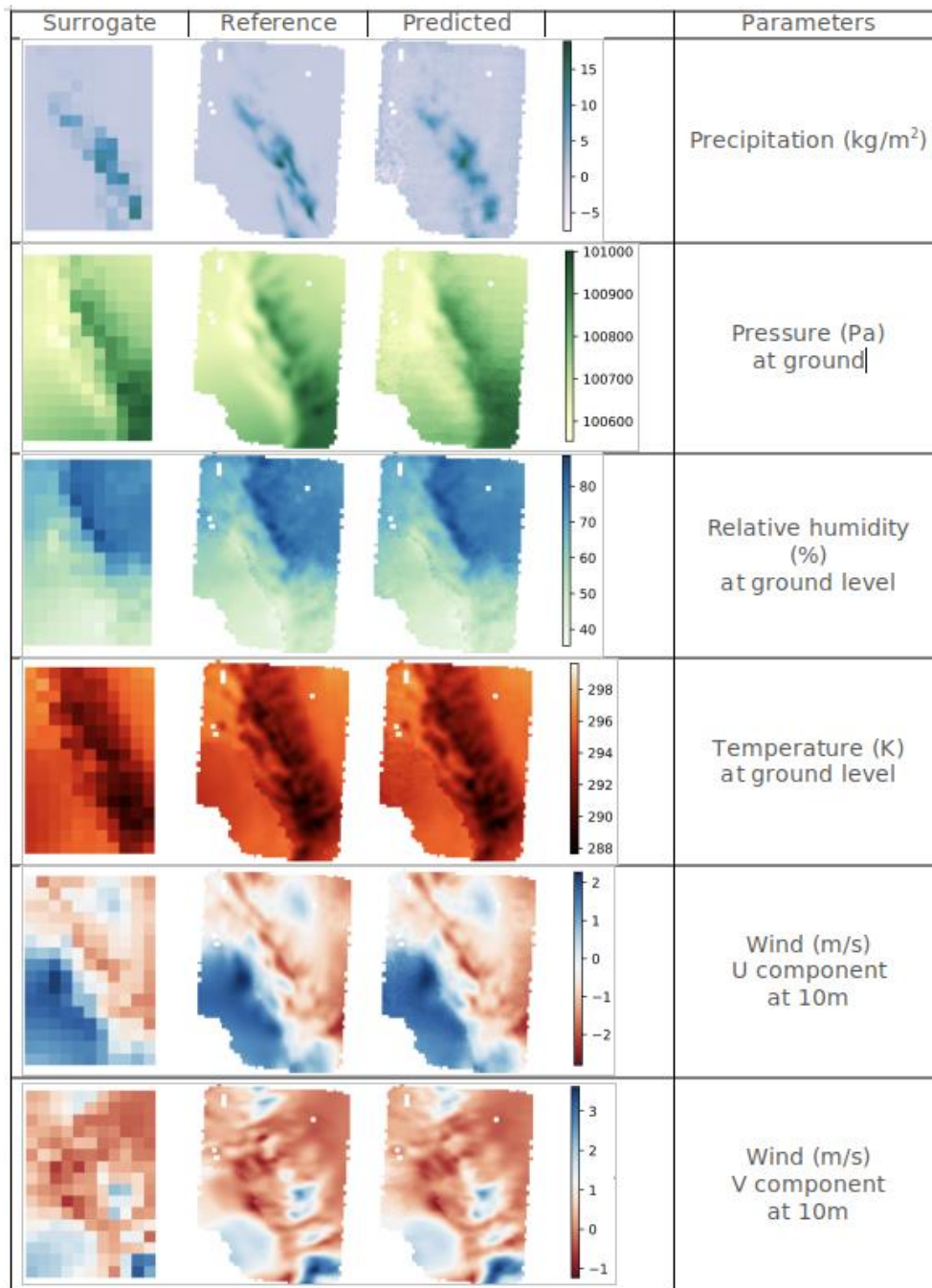


Figure 2.3. Examples of downscaled (i.e., predicted) atmospheric parameters with respect to the reference ones they should reproduce from the surrogate low resolution dataset. These are validation examples, it means that these data were not used in the training phase of the NN.





2.4. Mapping the surrogate dataset to the projection dataset

Figure 2.4 shows a comparison between the statistical distributions of the surrogate dataset and the projection past-subset (previously referred to as historical). We can see that there are clear shape similarities, but also very relevant differences at times (e.g. in the precipitation extreme values or in the RH higher values). This is not surprising because the surrogate dataset is an upscaling of a model result, run at higher resolution, so resolving physical phenomena schematised in the projection model.

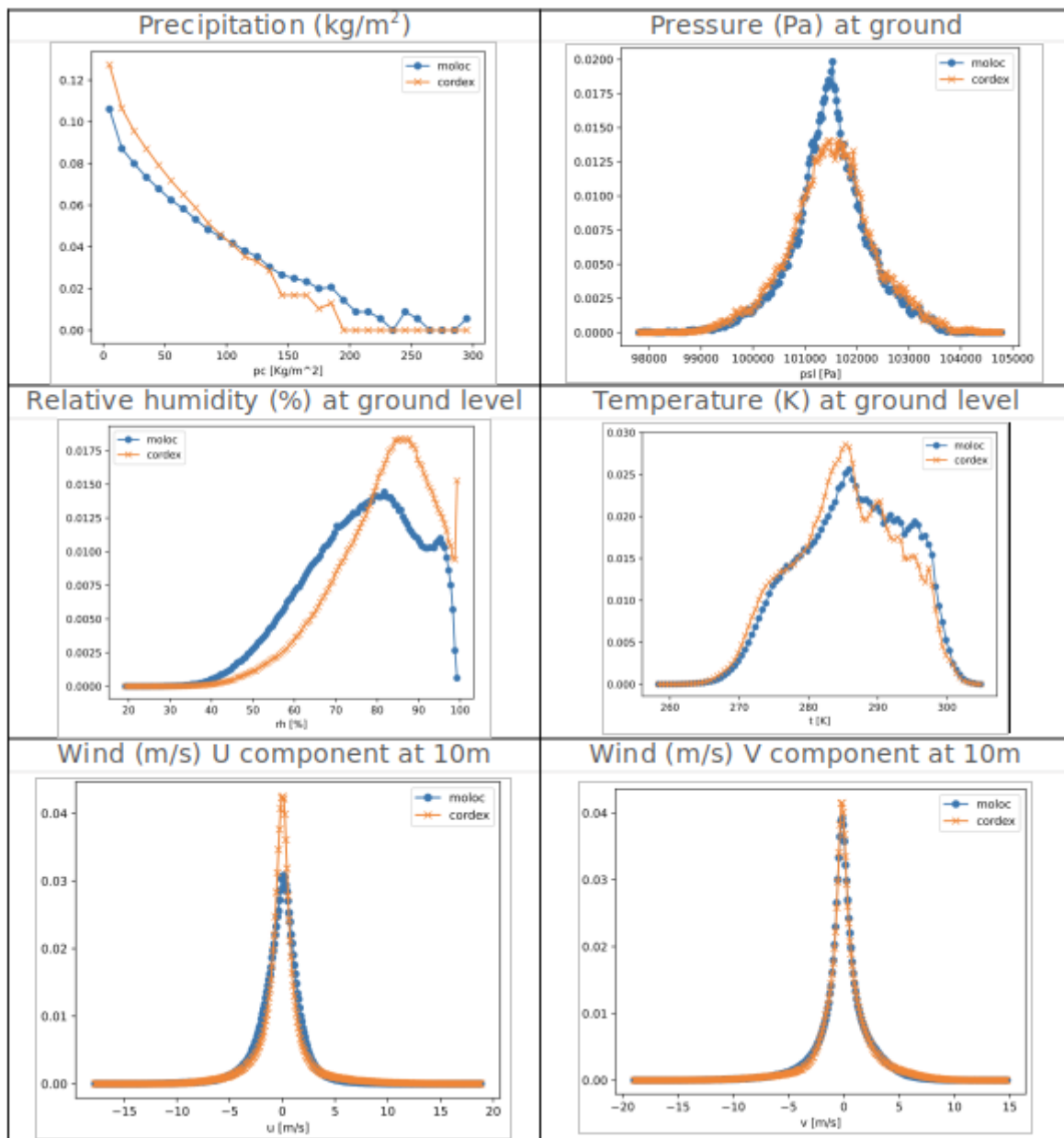


Figure 2.4. Comparison between statistical distributions of the surrogate dataset (Moloch) with the projection past-subset one (CORDEX).





It is apparent that is necessary to match these statistics, if we want to apply the NN downscaling relationships, (trained on the couple surrogate-reference data) to the projections. Now, we can proceed with the Probability Matching (PM) method, mapping Cumulative Distribution Functions (CDF's) to each other, through a step-by-step numerical integration process. In fact, given two CDF's on a closed interval, $F1(x)$, $F2(x)$, we can find a mapping $x \rightarrow g(x)$ such that the points x formerly distributed with CDF $F1(x)$, will now have distribution $F2(x)$. In other words, given some data distributed in a certain manner, we can find a transformation, that, when applied to our data, will result in data distributed according to another (given) distribution (see for instance Rosenfeld et al., 1993).

As an example for precipitation, it can be mathematically expressed by:

$$\int_{p_{s_{\min}}}^{p_s} D_s dp_s = \int_{p_{h_{\min}}}^{p_h} D_h dp_h$$

In this way we map any value of precipitation in the surrogate dataset (p_s) in a corresponding one in the historical dataset (p_h) according to the cumulative distribution function (seen as a cumulative probability function). The relationship gives the numerical function g to pass from one distribution to the other. Note that the h functions is always found, even if the variables are completely uncorrelated (see Figure 2.5). For totally independent variables this delivers completely nonsense results, when we use the method to force the retrieval of a relationship. On the contrary it turns out to be a powerful property when dealing with variables that we know beforehand are correlated from a statistical point of view, such as our atmospheric parameters from non-synchronised models in the surrogate and historical datasets.

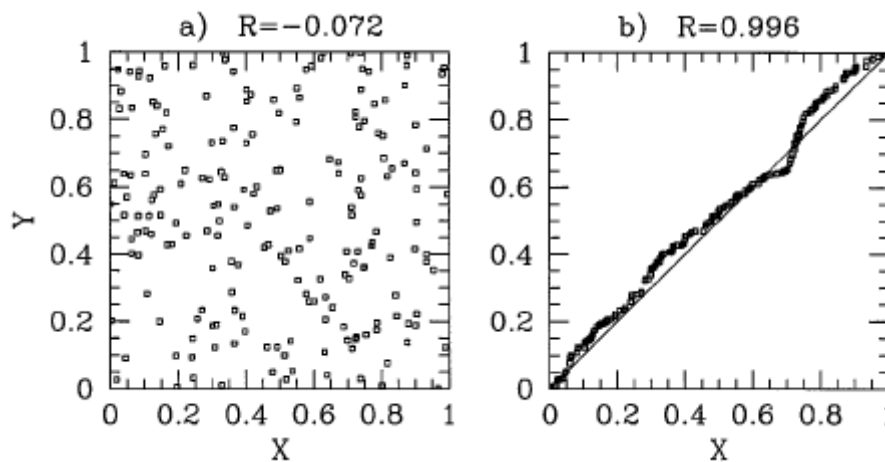


Figure 2.5. Left panel: (X,Y) couples that are randomly generated. Right panel: probability matching method applied to the couples of the left panel with the assumption they are statistically correlated. The resulting relationship is represented by the dotted line. In this case, as expected, dots are very close to the bisector line, being X and Y generated exactly with the same random process, thus with the same distributions.





2.5. The local downscaling process

In order to be able to generate projections for local atmospheric parameters, as measured by a local meteorological station (i.e. in a single, theoretically dimensionless, point), we have now developed two algorithmic tools, the NN and the PM ones, than can turn out to be useful for our purpose. Both in fact are capable to address the problem, even if the two methodologies are conceptually very different and the accuracy of the results are expected to be different accordingly.

The first one is the NN approach. In this case we can use the same NN structure described above, developed for connecting two different resolution datasets (the reference and the surrogate ones), that in the training phase had the property to be perfectly coherent, both spatially and temporally (being the surrogate dataset just the spatial upscaling of the reference one). Here, the most coherent (i.e. synchronised) datasets that we can have are a time series of past measurements from a given meteorological station (the ones that we want to produce the projection in the future), that becomes our reference data, and the evaluation subset of the projection dataset, provided that they have a significant temporal overlapping. We remind that, differently from the historical dataset, any evaluation dataset is obtained running a climatological model in the past, but forced by external data (including systematic global measurements), aimed at reproducing as much as possible the real sequence of atmospheric events with the correct timing. Thus, in this case they can be used instead of the surrogate dataset for training the NN against the meteo station data. Of course, after the training, we expect much greater differences between the NN predictions and the reference data (i.e. the meteo station time series), than for the couple surrogate-reference datasets of the spatial downscaling process. Note that a subset of 20-30% of the whole available overlapping data will be kept out from the NN training to be properly used for validation objectives. In this case, the NN will be simplified by the fact that we are not downscaling a map, but we are connecting some model data to spatially dimensionless measurements. In sum we will train the NN to connect the values of the model grid point containing the coordinates of our meteo station, with the station measurements. More precisely we will use not only such model grid point, but also its nearest neighbours, exactly as done for the spatial downscaling. The process will be however simplified, in fact there will be neither more final map reconstruction (with retrieved weights for the overlapping pixels), nor need to match statistical distributions through the PM method, because here we do not use any intermediate surrogate dataset, but we directly connect low resolution evaluation data (from the projection dataset) to the local measurements. The process is easier but also more "noisy" and we expect to need longer corresponding (i.e. overlapping) datasets, to cope with the expected larger errors in the matching process.

If this is not the case, an alternative approach that can be used is the PM one. In this case, we simply use the PM to match the probability distributions computed from an enough populated (and climatological significant) time series from the reference meteo station with the historical ones, for any parameter of interests. In this case we do not need any temporal synchronisation, and thus it is the only way to proceed in the cases we have no or not sufficient temporal overlap between the reference time series and the evaluation data. Here, not needing synchronisation, we prefer to use the historical data than the evaluation ones, because of the supposed greater similarity with the behaviour of projections, as already claimed when dealing with the spatial downscaling. We can apply the PM method to the entire datasets or we can think to differentiate for instance according to different seasons, or months or even different events, provided we





have in use some classification methods. Any differentiation can improve the matching accuracy and thus projection reliability, but, as a major drawback, it reduces the statistical population available for building our distributions, so this is something to take into account, when looking for some optimal compromise in the local downscaling process.





3. DOWNSCALING OF SEA LEVELS

Projections of future sea level changes are usually based on global (GCMs) or regional climate models (RCMs) predictions. However, the changes in shallow coastal regions or marginal seas, as the sub-basins of the Mediterranean Sea, cannot be fully resolved by GCMs. To improve sea levels predictions and to study the effect of climate change on extreme water level, at both regional and coastal scale, dynamical downscaling based on high-resolution ocean models needs to be performed (Rockel et al., 2015; Liu et al., 2016; Vousdoukas et al., 2016; Fagundes et al., 2020; Sannino et al 2022). The downscaling between ocean models based on structured mesh usually cannot exceed the size ratio between the coarse and finer model solutions, greater than 3 (Pham et al., 2016). Therefore, multiple procedures are required to ensure the correct spatial resolution necessary to reproduce the hydrodynamics at coastal scale (Trotta et al., 2017; Kamidaira et al. 2019). This is often strongly influenced by the complex bathymetric and morphological local characteristics. Alternatively, unstructured-mesh ocean models, commonly used for coastal modelling (Danilov, 2013), offer an efficient substitute to the computationally expensive multiple-downscaling-steps approach (Zheng et al., 2012). In fact, the cross-scale approach, typically characterizing this type of applications, allows to potentially cover, in one implementation, from the open-ocean to the near shore dynamics (Umgiesser et al., 2022).

3.1. Model description

To provide temporal sea level evolution data along the coast, a dynamic downscaling approach was decided to be followed in the SCORE project, which involves:

- 1) the use of an unstructured mesh hydrodynamic prediction model, with increasing resolution only near the area of interest (i.e., the marine area of each coastal city);
- 2) the use as atmospheric forcing (for wind and atmospheric pressure) of one of the atmospheric models available at the regional scale.

Such a dynamical downscaling application uses the SHYFEM model (Umgiesser et al., 2004), a high-resolution ocean model based on the finite elements method. In particular, the model is forced by atmospheric data from the RCM ALADIN 63 and from the EUROCORDEX project (Jacobs et al., 2014). See section 1.2.3 Methodology to downscale climate information.

In this section the SHYFEM model system is described along with the procedures necessary for its implementation, running and evaluation. The description of the numerical model, its application to the study site, the adopted simulations setup, and the post-processing procedure necessary for the analysis of the model outputs, are reported below.

SHYFEM (Umgiesser et al., 2004) is an open-source three-dimensional hydrodynamic model based on the finite elements method, widely used to reproduce the water circulation and the main hydrodynamics in coastal and shallow water areas (freely downloadable at <https://github.com/SHYFEM-model/shyfem>). Particularly suited for predicting extreme storm surge events, it constitutes the core of several oceanographic prediction systems mainly developed for Mediterranean waters, e.g. for the Venice Lagoon (Bajo et al., 2007),





for the Adriatic Sea (Ferrarin et al. 2019) and for the Bonifacio Strait in the western Mediterranean Sea (Cucco et al., 2012, Quattrocchi et al., 2021). SHYFEM resolves the three-dimensional primitive equations integrated over z-layers in their formulations with water levels and transports. It accounts for baroclinic, barotropic and atmospheric pressure gradients, Coriolis force, wind drag and bottom friction, wind wave radiation stress, nonlinear advection and vertical turbulent processes. Following the approach commonly used for operational prediction of storm surge events in the Venice Lagoon and Northern Adriatic Sea (Zampato et al., 2006; Bajo et al., 2007; Umgiesser et al., 2022), the model was applied in its 2D linearized version and by considering only the wind drag and the atmospheric pressure gradients as the meteo-marine forcing determining the sea surface elevation in the selected coastal site. The governing equations read as:

$$\frac{\partial U}{\partial t} - fV = -gH \frac{\partial \zeta}{\partial x} - \frac{gH}{\rho_0} \frac{\partial p_a}{\partial x} + A_H \left(\frac{\partial^2 U}{\partial x^2} + \frac{\partial^2 U}{\partial y^2} \right) + \frac{1}{\rho_0} (\tau_x^{surf} - \tau_x^{bot})$$

$$\frac{\partial V}{\partial t} + fU = -gH \frac{\partial \zeta}{\partial y} - \frac{gH}{\rho_0} \frac{\partial p_a}{\partial y} + A_H \left(\frac{\partial^2 V}{\partial x^2} + \frac{\partial^2 V}{\partial y^2} \right) + \frac{1}{\rho_0} (\tau_y^{surf} - \tau_y^{bot})$$

$$\frac{\partial \zeta}{\partial t} + \frac{\partial U}{\partial x} + \frac{\partial V}{\partial y} = 0$$

where ζ indicates the water level, U and V the the vertically-integrated velocities (total or barotropic transports) in x and y directions, f the Coriolis parameter, p_a the atmospheric pressure, g the gravitational constant, ρ_0 the standard water density, τ the stress term at the surface, the wind stress term, and at the bottom, the bottom friction term, $H = h + \zeta$ the total water depth, h the undisturbed water depth, A_H the horizontal eddy viscosity estimated following the Smagorinsky parameterization (Smagorinsky, 1993). Wind and bottom friction terms, related to the wind speed and current velocity respectively, read as:

$$\tau_x^{sur} = c_D \rho_a w_x \sqrt{w_x^2 + w_y^2}$$

$$\tau_x^{bot} = c_B \rho_0 u \sqrt{u^2 + v^2}$$

$$\tau_y^{sur} = c_D \rho_a w_y \sqrt{w_x^2 + w_y^2}$$

$$\tau_y^{bot} = c_B \rho_0 v \sqrt{u^2 + v^2}$$

with c_D as the wind drag coefficient, c_B the bottom friction coefficient, ρ_a the air density (w_x, w_y) the wind velocity (at 10 m above water level) components and (u, v) the horizontal velocity components.

The horizontal space integration is made with a finite element technique, using a staggered grid, while the integration in time is made through a semi-implicit scheme. The Coriolis force, the barotropic pressure gradient terms in the momentum equation, and the divergence term in the continuity equation are treated semi-implicitly, while all the remaining terms are treated explicitly. The model adopts automatic internal





substepping over time to enforce numerical stability with respect to advection and diffusion terms. Due to the semi-implicit scheme, a staggered grid formulation is necessary to conserve the mass of the system (Umgiesser et al., 2004). Accordingly, the water levels are computed on the vertices of a triangular mesh, while the velocities are computed at the centre of the triangles, using a step shape function.

3.2. Model implementation

To simplify the description of the implementation process, the case study of the coastal area surrounding the city of Massa in the Ligurian Sea (sometimes referred to as northern Tyrrhenian Sea) is described. To do that, the SHYFEM model system was applied to scale the CORDEX sea levels predictions made for both present day and future RCP scenarios. The Western Mediterranean Sea is characterized by a low tidal dynamics with amplitudes varying between a few cm up to 20 cm for the Tyrrhenian Sea (Alberola et al., 1995). Sea-level changes at decadal and interannual time scales are due to density and water-mass distribution variations in the ocean, driven by wind, atmospheric pressure, heat and water fluxes and barostatic sea-level changes through water-mass exchange between the land and the ocean (Bonaduce et al., 2020). Among all the different involved forcings, extremes inundations events are driven mainly by the action of the wind and waves, which exert a direct drag on the surface water masses, and by the atmospheric pressure gradients, which force the whole water column toward low pressures areas (Lionello et al., 2021).

The selected coastal site, facing at the western part of the Mediterranean Sea is mainly affected by north-westerly and southern winds, Sirocco and Mistral, both characterized by a limited fetch due to the geometrical features of the basin (Barbariol et al., 2021). Therefore, for this specific site, considering the potentiality offered by the unstructured-mesh ocean model, any nesting between the oceanographic component of the GCM and the coastal model was not necessary to reproduce the impact of storm events on the local sea water levels. The downscaling procedure was, in fact, applied considering only the predicted atmospheric fields as forcing for a coastal model implementation covering the whole Mediterranean Sea with a specific focus on the Tyrrhenian Sea. With this aim, a high-resolution computational mesh was then built with a varying spatial resolution adapted to satisfactorily reproduce the morpho-bathymetrical characteristics of the investigated coastal region. A set of hindcast numerical simulations were performed to evaluate the model performances in reproducing the sea surface surge induced by a set of severe storm events that occurred in the past decades. Finally, the calibrated and validated model systems were applied to make predictions of the water level set up in relation to both climatic and sea level rise future scenarios.

The simulation results correspond to the residual signal of the total water elevation obtainable, from observations, after de-tiding and detrending procedures. A further statistical procedure was therefore applied to account for both the astronomical and the other oceanographic contributions to the total water elevation.

The model predictions, along with the wave climate data obtained from the application of a phase-averaging wind-wave model for the same climatic scenarios, will be adopted as input data for a high-resolution flow and wave model, to compute the combined effects of wind and wave setup on the inundation of the near-shore zones.





3.2.1. Numerical mesh

SHYFEM integrates the equation system on a finite element mesh, an unstructured grid composed of triangular elements of different size and form. For this application, different model meshes were designed and implemented in order to detect the most suitable configuration of the model domain for the purpose of this study.

The GMSH, an open-source software based on the Delaunay triangulation algorithm (<https://gmsh.info>) was adopted to build the model meshes. Highly detailed geometrical and bathymetrical data of the study site corresponding to the trait of coastal sea in proximity of the city of Massa (44°00'33.8"N 10°06'06.9"E) in the Tuscany Region, Italy, were used as input for the meshing procedure.

Considering the scope of the model application to reproduce the atmospheric component of the total water elevation during storm surge events, and the fetch of the main wind regimes acting in the area, the model domain should necessarily extend to the whole Tyrrhenian Sea and part of the Western and Central basins. With this premise, a total of 8 different unstructured meshes were constructed to test the model's efficiency and accuracy.

In Figure 3.1, the numerical grids are depicted along with indications about the ratios behind this choice. The adopted strategy can be summarized in testing the role of spatial resolution and domain configuration on the computational costs and model accuracy. Therefore, the numerical domain was alternatively extended to the whole Mediterranean Sea (MED), or limited to the West and central part of the Mediterranean basin only (WMED). For both MED and WMED groups, a relative increment of the spatial resolution was imposed for the coastal study site, whereas specific increments were applied for the whole domain, in the case of the MED group, and along the main wind fetches only, in the WMED case.

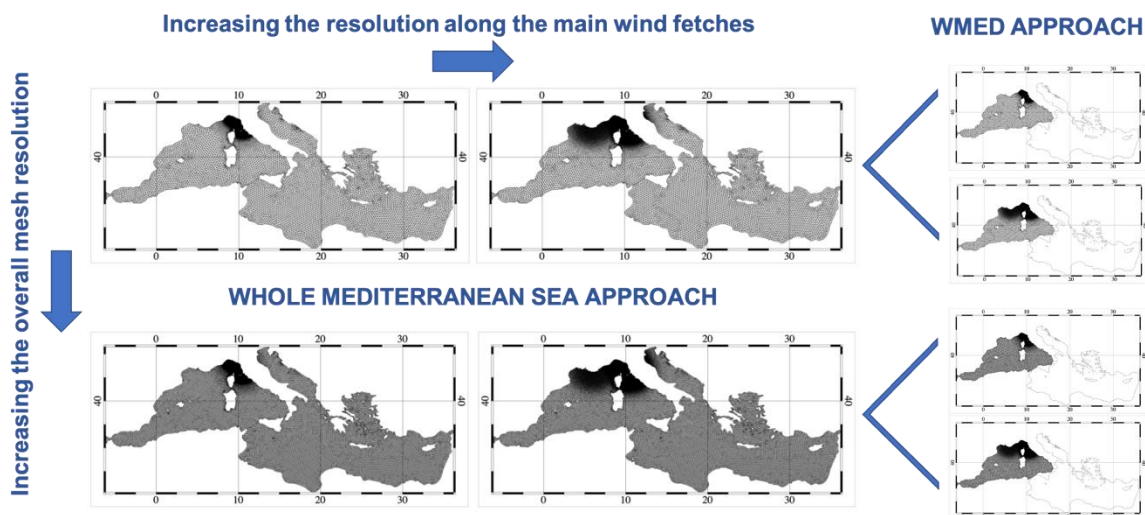


Figure 3.1. The 8 finite element meshes, grouped into the “MED” and “WMED”, adopted for testing the numerical model. Arrows and lines support the interpretation of the selected numerical strategies.

The number of computational nodes varied roughly between 30000 to 100000 with spatial resolutions ranging between 25 and 10 km for the open ocean and from 1200 to 400 m for the shelf area in front of the study site, for the meshes with the lower and higher resolutions, respectively. For all the cases, the finest





resolution was always imposed in correspondence to the interested coastal area with a minimum element size of 100 m.

3.2.2. Atmospheric forcing and ocean data

Wind and atmospheric pressure data provided by the CORDEX project were used as model surface boundary conditions. The dataset covers the whole Mediterranean Sea and part of the eastern Atlantic Ocean and is characterized by a spatial resolution of 0.1° and by a 3-hour temporal frequency. The data are constituted by the horizontal components of the wind speed at 10 m above the sea level, expressed in m/s, and by the atmospheric pressure expressed in Pascal. In the first phase of the study the atmospheric data computed for the biannual 2011 and 2012 was used for preliminary testing the model results. This evaluation period was selected in relation to the occurrence of intense storm surge events to be used as a test case for the calibration of the model parameters and for the assessment of the accuracy of the numerical prediction. The forcing dataset was preprocessed converting the grib format of the native files into the SHYFEM format consisting in binary file with structure well described in the model manual (freely downloadable at <https://github.com/SHYFEM-model/shyfem>).

For the same period, the observed sea surface elevation obtained from tidal gauge located in proximity of the study site was collected and processed. The two year length time series of the total sea surface elevation was preliminary processed to separate the contribution of the wind and atmospheric pressure from the astronomical one. Specifically, the dataset was detrended and filtered out of the tidal contribution by applying a commonly used de-tiding algorithm (Pawlowicz et al., 2002). As the astronomical contribution was quite low with respect to the total level, a further 12-hours mobile averaging was applied to the de-tided signal to account for all the possible masked semidiurnal components, which is the dominant tidal frequency in the area. The obtained residual signal, thus representing the contribution of atmospheric forcings on the sea water elevation, was then analysed to detect extreme storm surge events during the interest period. In Figure 2 the results obtained by the filtering procedure are depicted for the period between the 20th October to 25th November 2012 when several severe storm surge events impacted the Massa littoral.

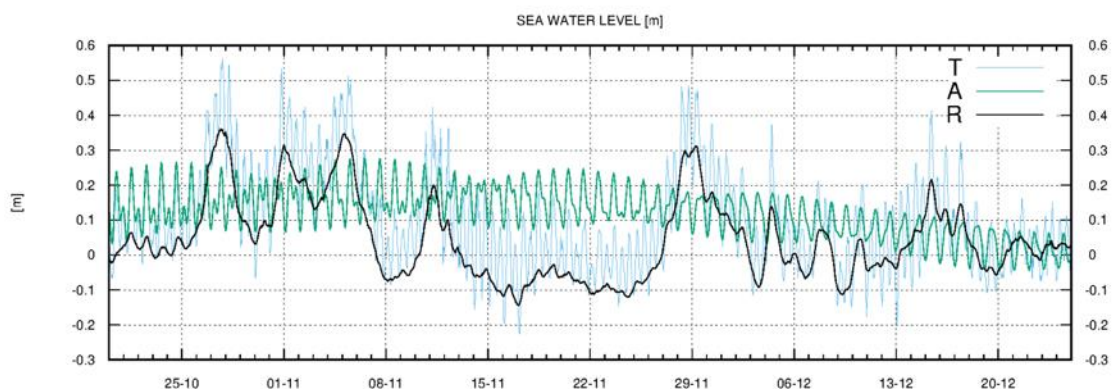


Figure 3.2. Total water elevation (T) with astronomical contribution (A) and residual signal [®] measured at the Massa tidal gauge between 20th October and 25th November 2012.





The residual sea surface elevation was considered as the observational dataset to be used for testing the model accuracy in reproducing the effect of the meteorological forcing on the sea surface elevation.

3.2.3. Model and simulation setup

SHYFEM version 7.5.71 (downloaded at <https://github.com/SHYFEM-model/shyfer>) was installed and ran in serial mode on Linux UBUNTU-based workstation, following the procedure described in the manual. In this initial phase, the model was applied in a series of yearly simulation runs to test the computational cost and its sensitivity to the main parameters. Specifically, the effects of the mesh configuration, time stepping and wind drag and bottom friction formulation was analysed by means of a sensitivity analysis. Numerical simulations were carried out to reproduce the sea water elevation during the year 2012. At each model run, the previously listed set of options and model parameters were modified and the Root Means Squared (RMS) error in reproducing the observed residual water levels was estimated.

SHYFEM adopts the quadratic formulation for describing both the wind drag and bottom friction contribution to the momentum equations. Among the possible approaches to define the friction parameters c_B and c_D , we considered both constant in time, homogeneous in space, and temporally and spatially variable formulations. In particular, a constant and homogeneous formulation of the bottom coefficient c_B was selected with typical values ranging between 10^{-3} and 10^{-2} , whereas both constant and wind-speed-dependent formulas were tested for estimating the optimal Wind Drag coefficient c_D . In the first case c_D was varied, similarly to the bottom friction, between 10^{-3} and 10^{-2} , while the Smith & Banke (1975) and Large & Pond (1981) formulas were considered for the temporally and spatially variable approach.

3.3. Output data description

The model outputs consist of a full year hourly sequence of sea surface elevation fields over the entire numerical domain. For each model run, the dataset is further processed to extract the time series of the water levels in correspondence to the tidal gauge of Massa (more precisely of Marina di Massa), to compute the discrepancies with the observations. Figure 3.3 shows an example of the sensitivity run outputs for two different simulations where, considering the standard constant formulation for both c_D and c_B , the MED (purple line) and WMED (green line) mesh approaches were tested and compared with the observed residual levels (black line).

From a preliminary qualitative evaluation, the obtained model results considering the whole Mediterranean Sea as model domain, better reproduce the observations, especially when intense storm events hit the coast (peak levels in Figure 3.3).

The model outputs also can be visualized in the form of hourly maps of sea water elevation, to investigate the extent of the surge phenomena helpful to modify and optimize the mesh configuration and resolution. As an example, Figure 3.4 shows the results obtained from a simulation-run based on the MED configuration mesh, mapping the sea surface elevation over the entire domain (left panel of Figure 3.4) and for a zoom on the interested area (right panel of Figure 3.4) in the moment (29th November 2012 at 1:00 a.m.) a relative maximum of the residual elevation was observed. From the model results it is clear the surge effects mainly interest the coastal area with an extremely localized peak in proximity to the study site (yellow star in the





map). This type of evaluation has been preliminary used to detect which part of the model domain needs specific adjustment of the mesh spatial resolution to better reproduce the storm surge dynamic.

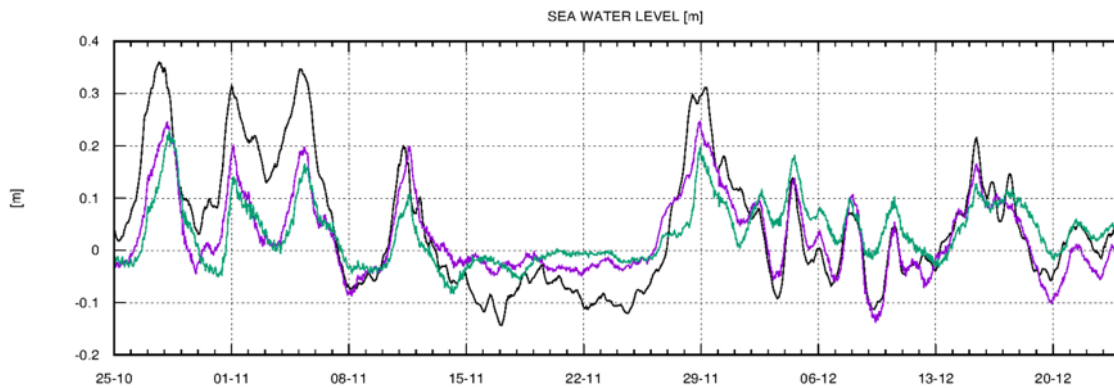


Figure 3.3. Observed (black line) and modelled (colored lines) residual water levels at the Massa tidal gauge between 25th October and 25th November 2012. Purple and green lines refer to numerical results obtained by MED and WMED mesh simulation runs, respectively.

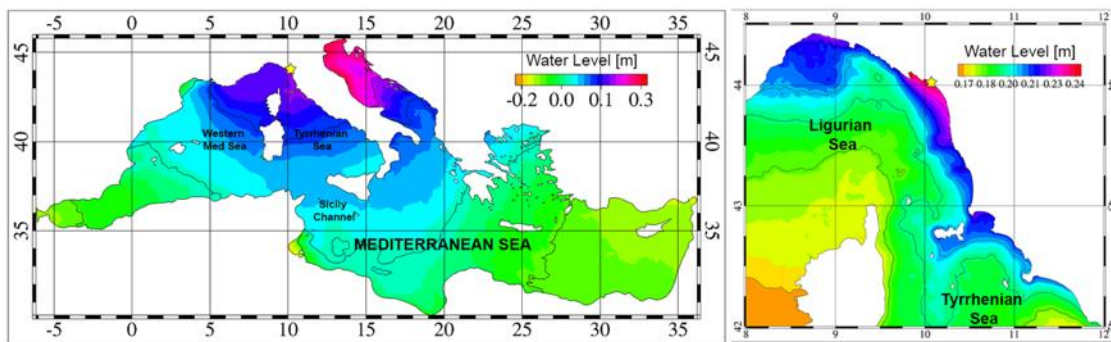


Figure 3.4. Sea surface elevation obtained from numerical simulation running the MED mesh type for the 29th November 2012 at 1:00 am. Left panel depicts the results over the whole model domain whereas, while in the right panel, a subset focus on the interested area is reported. Yellow star indicates the location of the tidal gauge.

The results obtained by simulation runs of both hindcast and forecast simulations will be analysed on the basis of the previously described visualization and processing strategy.





4. DOWNSCALING OF WAVES

The downscaling of the wave climate is important for several applications ranging from extreme value analysis (Coles, 2001), coastal vulnerability assessment, and long-term analysis of erosion/progradation trends.

All these applications require a high-resolution modelling of wave climate, in order to account for the bathymetric characteristics of the area and the shape of the coastline. To this aim, the use of numerical models on unstructured grids is essential.

For the present task we use the third generation spectral wave model WWIII, which represents the state of the art of the wave climate modelling and is implemented on unstructured grids (WWIII Development group, 2016).

4.1. Model description

Wave propagation, or the propagation of spectral components representing the sea state at a given point, is described by a number of parameters characterizing phase and amplitude. Among the phase parameters, the most important are the wave numbers k (or its vector form following the direction of the wave at that point), the ϑ direction (perpendicular to the wave crest), and the frequency. The latter can be expressed in various forms, as relative frequency σ (the frequency observed from a reference system integral with the average current), or as absolute frequency ω (the frequency observed from a fixed reference system)

$$\sigma = 2\pi f_r$$

$$\omega = 2\pi f_a$$

Under the geometrical optics approximation (slowly varying current and depth), the quasi-uniform (linear) wave theory can be applied locally, giving the classical dispersion relation and Doppler-type equation:

$$\sigma^2 = kg \tanh kh$$

$$\omega = \sigma + k \cdot U$$

where h is the mean water depth and U is the current velocity (depth- and time- averaged over the scales of individual waves). A major assumption is that for slowly varying depths and currents some interaction can be ignored, including wave diffraction, scattering and interference effects. As from the usual definition of k and ω from the phase function of a wave, the number of wave crests is conserved (see, e.g., Phillips, 1977; Mei, 1983):

$$\frac{\partial k}{\partial t} + \nabla \omega = 0$$

From such equations the rates of change of the phase parameters can be calculated.

The representation of irregular waves is synthesised by the so-called energy spectrum F which represents the random variance of the sea surface. This spectrum F is a function of all independent phase parameters,





i.e., $F(k, \sigma, \omega)$, but, as in most cases the three frequency parameters are interrelated, normally it is assumed $F=F(f, \vartheta)$ or $F=F(k, \vartheta)$, and the different spectra can be calculated using Jacobian transformations.

In a general cases with currents, the energy or variance of a wave packet is not conserved due to the work done by the current on the mean momentum transfer of waves (Longuet-Higgins and Stewart, 1961, 1962). However wave action $A \equiv E/\sigma$ is conserved (e.g., Whitham, 1965; Bretherton and Garrett, 1968), so the wave action density spectrum $N(k, \vartheta) \equiv F(k, \vartheta)/\sigma$ is normally used within models. Wave propagation then is described by:

$$\frac{DN}{Dt} = S$$

where D/Dt represents the total derivative (moving with a wave component) and S represents the net effect of sources and sinks for the spectrum. As it is generally assumed that wave propagation is linear and without scattering, nonlinear wave-wave interactions are part of the S term, as well as partial wave reflections.

The inclusion and calculation of nonlinear terms is one of the elements that has most characterised the development of wave prediction models: the first generation models did not calculate these effects, while in the second generation models these effects were taken into account through parameterisations. Finally, in the third-generation models, from the second half of the 1980s onwards, non-linear wave interactions are tightly described through approximate or even exact formulations. In the most general case, the source terms include multiple effects:

$$S = S_{in} + S_{nl} + S_{ds} + S_{bot} + S_{db} + \dots$$

- S_{in} , is an energy input due to atmosphere-wave interaction term (wind) and is usually a positive (negative in the case of swell);
- S_{nl} represent nonlinear wave-wave interactions;
- S_{ds} represents wave-ocean interaction dissipative term that is generally dominated by wave breaking;
- S_{bot} represents wave-bottom interactions in shallow water;
- S_{db} describes additional shallow water dissipative processes in extremely shallow water (wave breaking due to wave-bottom effects).

Other source term may include: triad wave-wave interactions (S_{tr}), scattering of waves by bottom features (S_{sc}), wave-ice interactions (S_{ice}), reflection etc.

The outputs of the models include the significant wave height, information regarding the period (mean, peak), associated direction, and most of all spectral information regarding the energy distribution at different wavelengths. The models that have a longer history of operational implementations are WAM and WWIII.

The WAM, developed by the Wave Model Development and Implementation Group (WAMDI), has been operational since 1992 at the European Centre for Weather Forecasting (ECMWF) for real-time wave prediction from global to basin scale.

WAVEWATCH III (<https://github.com/noaa-emc/ww3>), referred to as WWIII, is a community wave modelling that includes some of the latest scientific advancements in the field of wind-wave modelling and dynamics. WWIII differs from its predecessors in many different points such as equations, model structure, numerical methods and parameterisation of physics. WWIII is the model chosen within SCORE for wave climate





projections. This is both because there is long experience within the SCORE partnership in using this model, and because the recent formulation of this model to be used on an unstructured mesh grid allows the flexibility of use that is needed to calculate effects at local and coastal scales.

4.2. Model implementation

The process described here can be considered as an example for the implementation of the WWIII model in the Mediterranean Sea with four case studies corresponding to the coastal areas surrounding the cities of Benidorm (Spain), Vilanova (Spain), Massa (Italy), and Piran (Slovenia). In general, the implementation of the model follows a series of steps, which are briefly described here. The user manual for the model is in fact quite detailed and the code itself is written in a very clear and readable manner. The various steps must be taken sequentially (through the use of different programmes that are compiled individually):

- A first step is related to the definition of the calculation grid and bathymetry;
- A second step involves the preparation of the atmospheric forcing;
- A final step, where the numerical and physical parameterizations are chosen, the model is compiled (WWIII can be run in a parallel manner following various standards depending on the computing machines used), the initial and boundary conditions, and the output variables, are chosen.

4.2.1. Numerical mesh

Although the Mediterranean Sea can be considered a closed basin at first approximation, the extent of the computational domain of the wave model includes the entire Mediterranean basin and an additional area 150 km west of the Strait of Gibraltar. This is done to improve accuracy in the Alboran Sea. The western limit of the domain is considered closed. This domain has been discretized by an unstructured mesh with a variable resolution up to 500 m in the coastal areas surrounding the above mentioned Mediterranean cities. The resolution decreases in the rest of the Mediterranean Sea, and the minimum resolution in deep offshore areas reaches about 60 km (see, Figures 4.1, and 4.2). In Figure 4.2, an unstructured mesh for the Black Sea is also shown.

As for the spectral domain, it spans 36 directions and 30 frequencies, which are not equally spaced, ranging from 0.0418 to 1.1181 Hz with a 12% increments.

The EMODnet bathymetry version 2018 was employed for the whole domain. In the Tuscany and Ligurian areas, data from available bathymetric surveys and nautical charts replaced the EMODnet bathymetry for average depths lower than 100 m. A minimum water depth of 4 m was set offshore and a constant water depth of 2 m was set in the wet grid points along the coastline in order to avoid numerical instabilities.

In order to verify the accuracy of the wave simulations in the high resolution zones, some climatological case studies were carried out in the Massa area and the results obtained with this grid were compared with those obtained with the higher resolution grid used in ref. [24] for an ERA5 reanalysis (Figure 4.3). In that case, where the time steps used were also shorter, and the computation time was clearly much longer, the domain was discretized by an unstructured mesh with a variable resolution up to 500 m along the coasts on the





North-Western Mediterranean Sea. The highest coastal resolution was dedicated to the coasts of Tuscany and the Tuscan Archipelago, Eastern Liguria (La Spezia-Levanto area) and the Straits of Bonifacio and Messina. Along the coasts of Sardinia and Corsica, the resolution was about 1 km; along the other Tyrrhenian coasts and on the Straits of Gibraltar, it was about 3 km; while for the remaining Mediterranean coasts, it was roughly 6 km. The minimum resolution in deep offshore areas reached 30 km. The differences between the results obtained using the two grids are negligible.

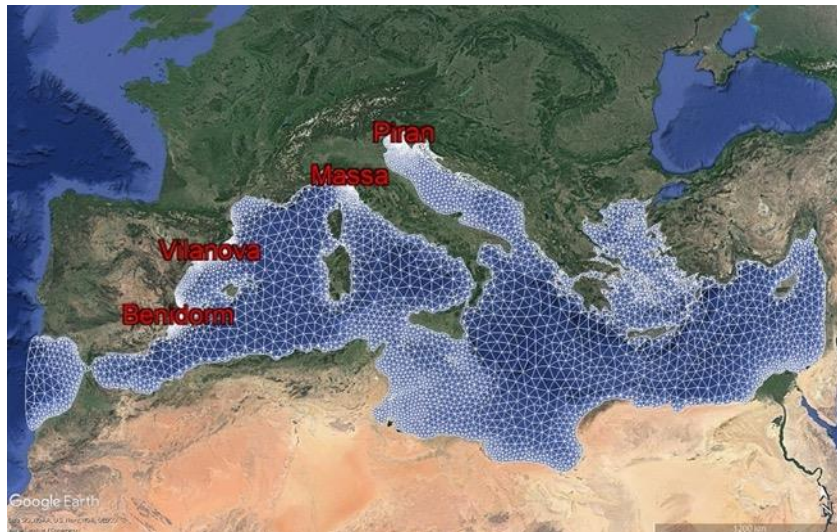


Figure 4.1. WWII grid of the Mediterranean Sea, showing coastal cities with higher resolution areas.

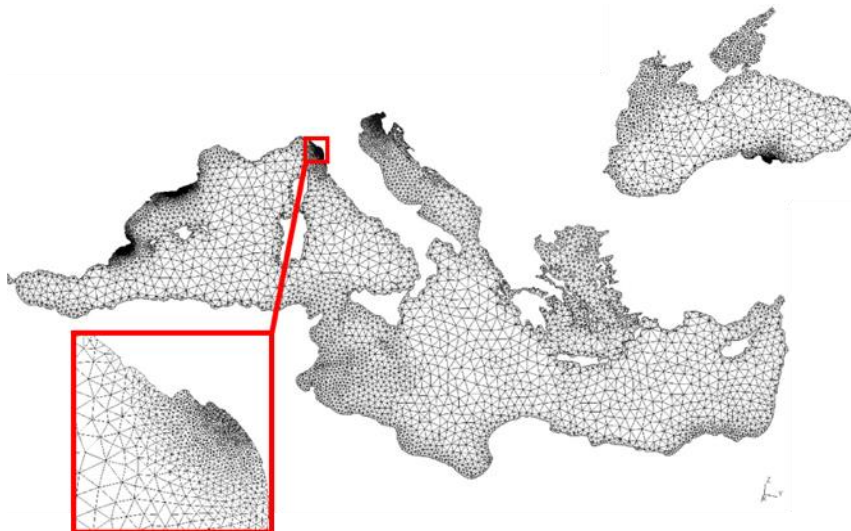


Figure 4.2. WWII grid of the Mediterranean Sea (the part outside the Strait of Gibraltar has been cut here) with an enlarged view of Marina di Massa. An example of an unstructured grid of the Black Sea is also shown.



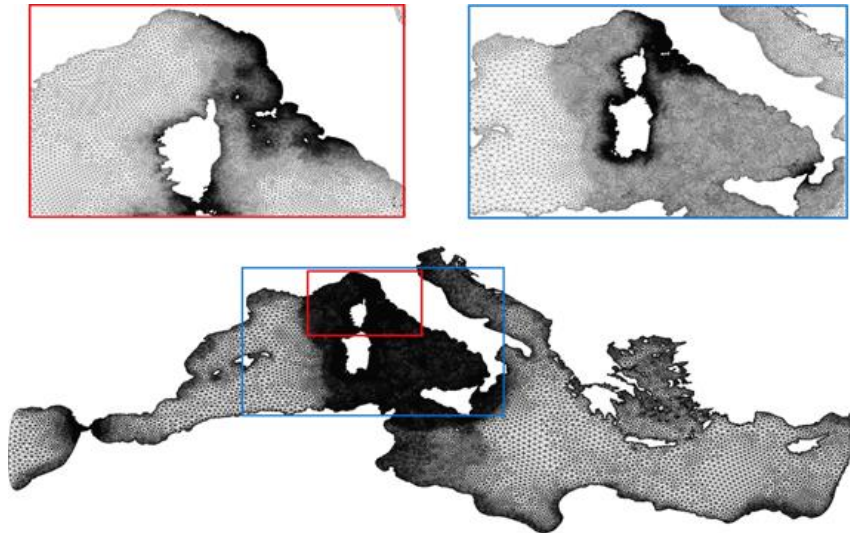


Figure 4.3. WWIII grid of ref. [24] with enlarged views of North-Western Mediterranean Sea (light blue box) and Tuscany Archipelago and Eastern Ligurian Coast (red box).

4.2.2. Atmospheric forcing

Wind data provided by the CORDEX project are used as wave model forcing (e.g. evaluation, historical, rcp4.5, rcp8.5). The dataset covers the whole Mediterranean Sea, the Black Sea, and part of the eastern Atlantic Ocean, and is characterized by a spatial resolution of about 0.1° and by a 3-hours temporal frequency. The data are constituted by the horizontal components of the wind speed at 10 m above the sea level, expressed in m/s. In the first phase of the study, the atmospheric data computed for the evaluation period (1979-2018) were used for a preliminary test of the model (calibration of the model parameters, and validation, i.e. the assessment of the accuracy of the numerical prediction). The forcing dataset was preprocessed via CDO (Climate Data Operator) and NCO (NetCDF Operators) routines by regridding the original NetCDF data, through Lambert conformal conic projection, into a regular NetCDF grid compatible with the WWIII NetCDF module. For more efficient processing, the wind data has also been divided into daily files (both with 24 time steps, 00h-23h, and 25 time steps, 00h-00h).

4.2.3. Model and simulation setup

Before compiling the model, it is necessary to make a number of choices concerning the numerical propagation schemes to be adopted, the parameterisations chosen for the source terms, and the way in which the non-linear interactions are calculated. These choices are based on a calibration process, which can be carried out in three subsequent phases by comparison of statistics from simulated and observed wave patterns, including both calm and severe weather conditions. Each phase corresponds to the calibration of a specific parameter/setup, namely: (i) time step duration, (ii) numerical scheme and (iii) physical parameterizations. For each, the calibrated parameter/setup is chosen on the basis of the best agreement between modelled and observed data.





In the final configuration, the maximum global time step is set equal to 240 s, whereas the maximum Courant–Friedrichs–Lewy (CFL) time steps for x - y and k - $theta$ were set equal to 60 s and 120 s, respectively. The minimum source term time step was set to equal 5 s (see ref. [24] for a comparison with the time steps used in the ERA5 simulations). The numerical scheme used is the explicit N scheme (1st order), as this scheme is considered the most efficient even if it suffers from an excessive diffusion. However, this diffusion can compensate for the possible garden-sprinkler effect when, for example, the waves travel around islands surrounded by deep water. Nonlinear wave–wave interactions were modelled using the discrete interaction approximation. The wind–wave interaction term (S_{in}) and the dissipation due to wave breaking (S_{ds}) were implemented with the source term package ST4 of WWIII.

As for the initial conditions, after a cold start, the model is reinitialized with a daily restart file. Therefore, if the simulation-run crashes, it can be restarted from the last simulated day. As far as the boundary conditions are concerned, the domain is simply considered closed.

The results of the model have been finally validated for the Massa area, through a comparison with some buoys in the Ligurian and Tyrrhenian seas.

4.3. Output data description

The output of the wave model is recorded hourly at all grid points for the integrated quantities: significant wave height (H_s), mean wave period (T_m), peak wave period (T_p), mean wave direction (Dir_m) and peak wave direction (Dir_p).

The output is also recorded hourly in 67 points for both mean and spectral wave parameters. Part of these points coincide with the locations of some buoys in the Ligurian and Tyrrhenian seas, while the others are located along the coast in front of Benidorm, Vilanova, Massa, and Piran (about 12-14 points for each city). About half of these latter points are located at a distance of 1 km from the coast, the others at a distance of 5 km (see Figure 4.4). Mean wave parameters at the points corresponding to the positions of the buoys were used for model calibration and validation.

Figures 4.5 and 4.6 show a comparison between the significant wave height data of Gorgona and La Spezia buoys and those of WWIII with Med-CORDEX Evaluation forcing. The correlation between the two dataset is very good, but an underestimation of the significant wave height is also evident, mainly due to the low resolution of the Med-CORDEX winds (see, for example, ref. [24] for a comparison with results obtained with high resolution winds).



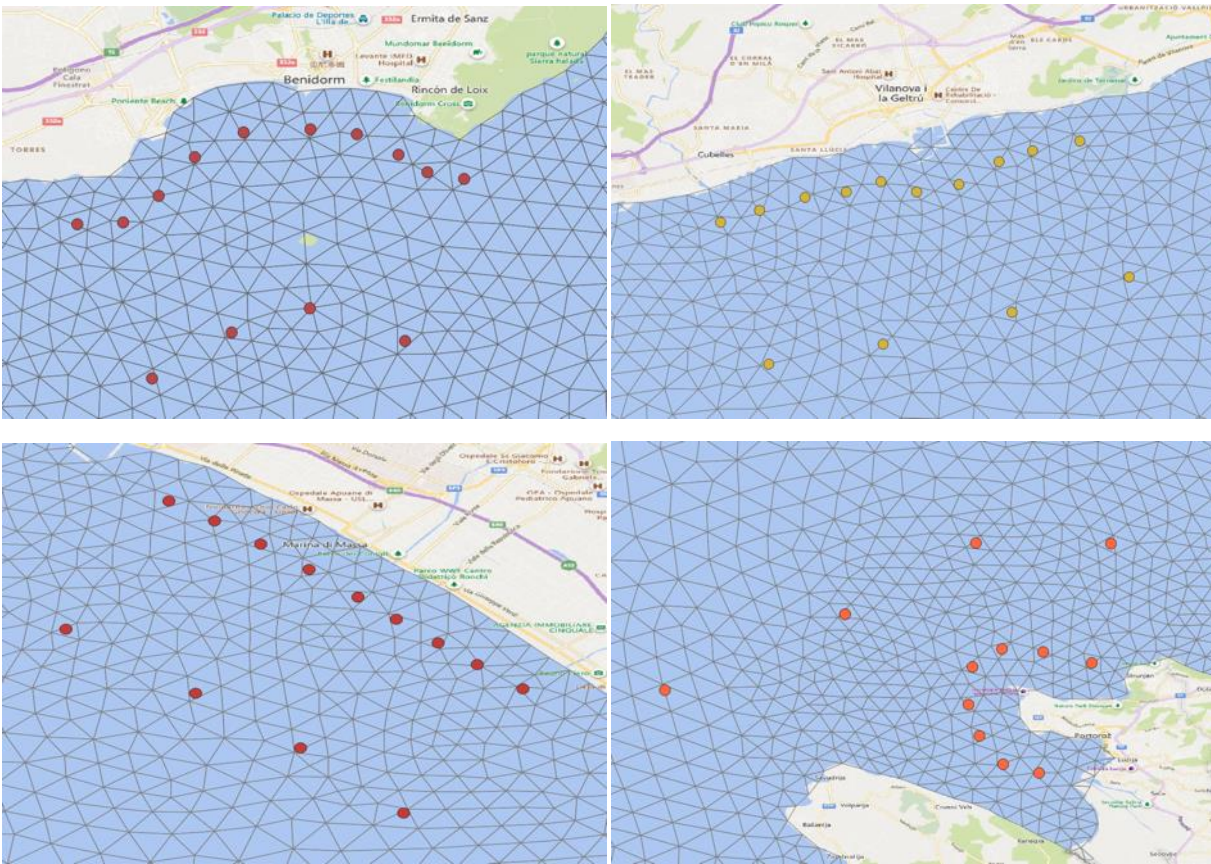


Figure 4.4. Positions of the points for the output of the wave spectrum parameters in front of Benidorm, Vilanova, Massa and Piran.

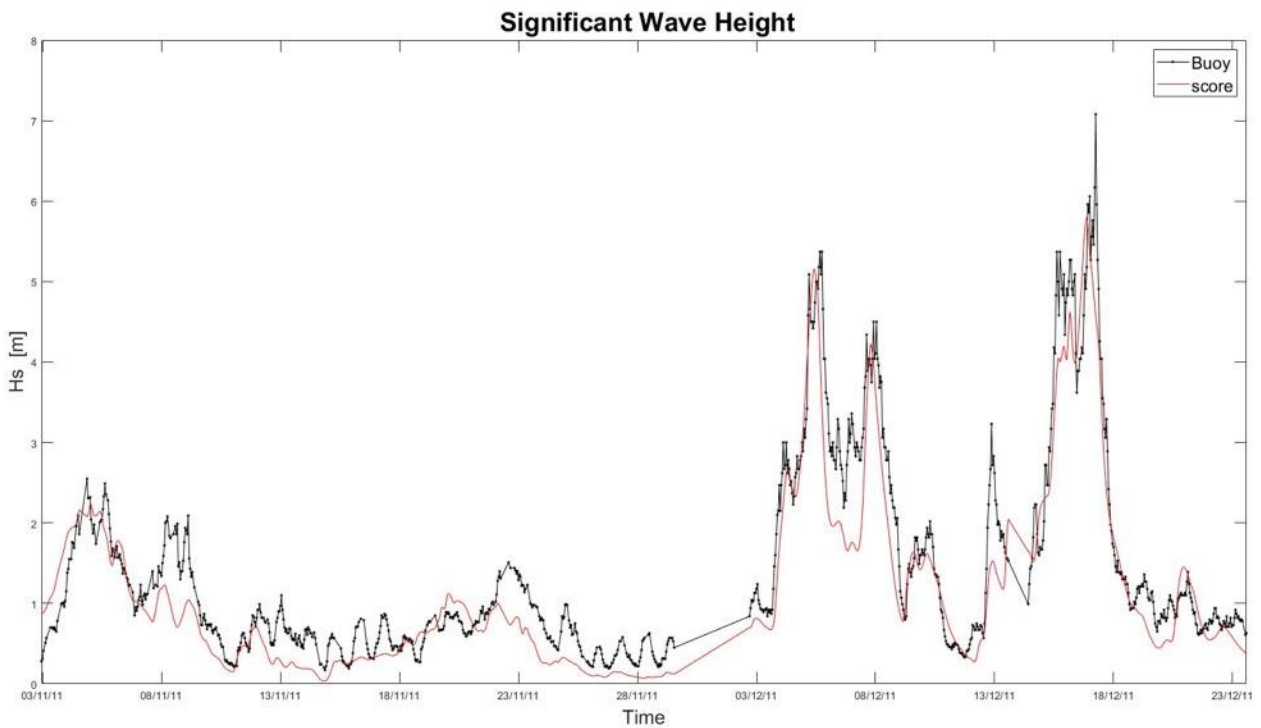


Figure 4.5. Comparison between Gorgona buoy data (black) and WWIII data (red) with Med-CORDEX Evaluation forcing.



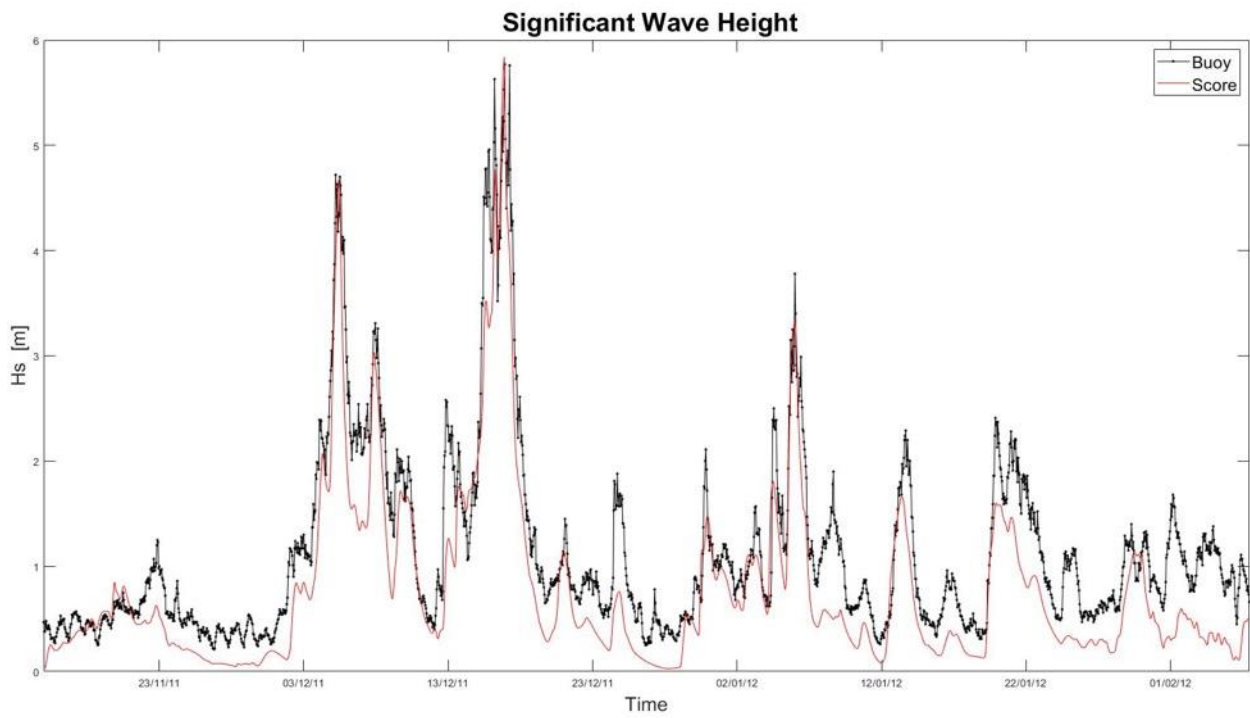


Figure 4.6. Comparison between La Spezia buoy data (black) and WWIII data (red) with Med-CORDEX Evaluation forcing.

In Figure 4.7, the model output in the form of an hourly map of significant wave height is also shown.

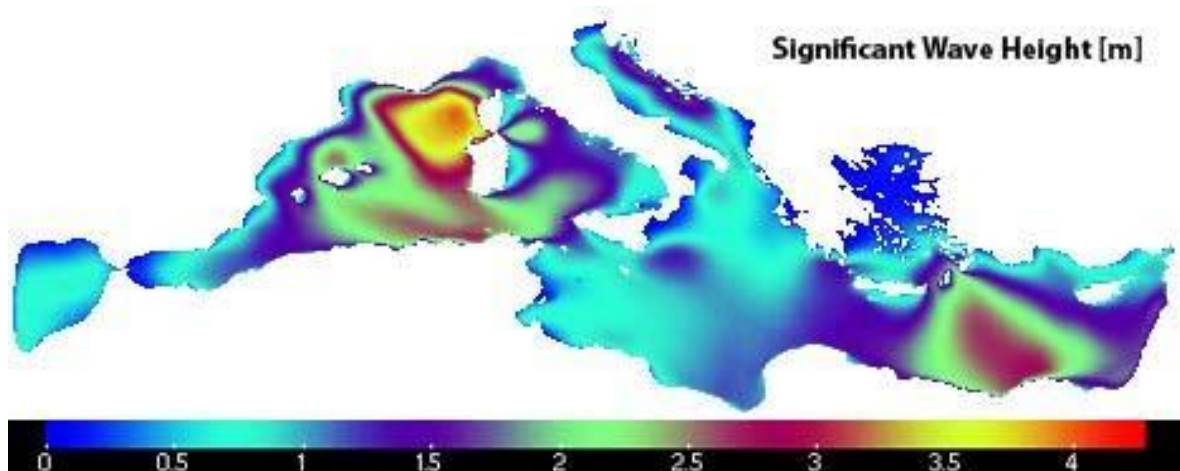


Figure 4.7. Hourly map of significant wave height.





5. HYDROLOGICAL DOWNSCALING

5.1. Hydrological models as a downscaling tool

River floods occur when the stream or channel geometry is not sufficient to contain the incoming volume of water. In order to model river floods, it is necessary to define the discharge hydrographs, i.e. the evolution in time of flow rate in given cross sections. The shape of the hydrograph, the time and value of its peak, and in general the streamflow generated in the channel network as a response to precipitation events, are the consequences of the hydrological processes in the upstream basin.

Such processes include several complex mechanisms occurring at the land surface (infiltration, evapotranspiration, runoff generation, hillslope routing, snow melt, groundwater recharge, ...) that depend on the geomorphological characteristics of the basin, soil hydraulic properties, and land cover. Hydrological models can be used to simulate these processes. Different approaches can be used, from simple empirical models to distributed physically-based models where the terrain is represented by a gridded domain, and dynamic equations for the various hydrological processes are implemented.

Within the framework of the SCORE project, hydrological models will be implemented for the river basins pertinent to the selected frontrunner cities, with EUROCORDERX projections of atmospheric fields as meteorological input (the same climate scenarios of those used for marine models). This will allow us to define the expected hydrographs for events with associated probability of occurrence in a climate change scenario, that will then be used into the urban-scale hydraulic model for the computation of flooded areas. Hydrological models can therefore be seen as downscaling tools since they serve the purpose of deriving information relevant at local/urban scale, i.e. discharge hydrographs, from meteorological data at regional scale (EUROCORDERX).

Among the various hydrological models available, we propose to use the LISFLOOD model developed by the Joint Research Centre (JRC) of the European Commission (<https://ec-jrc.github.io/lisflood/>) for several reasons:

- it has been applied in different contexts in Europe and worldwide and is used for example in EFAS (European Flood Awareness System) and GloFAS (Global Flood Awareness System);
- its code is freely available;
- it is a very complete model that can be used and customised for different applications;
- its implementation requires considerable efforts in terms of data preparation and model set up, compared to simpler models or commercial packages, but we believe that once this initial step is consolidated, the acquired know-how can be successfully used for many other applications.

5.2. LISFLOOD model

LISFLOOD is a spatially distributed water resources model, developed by the Joint Research Centre (JRC) of the European Commission since 1997. It has been applied to a wide range of water resources applications





such as simulating flood prevention and river regulation measures, flood forecasting, drought and soil moisture assessment and forecasting, the impacts of climate and land-use changes on water resources, and the impact of various water efficiency measures on water resources.

The model has been designed to be applied across a wide range of spatial and temporal scales. LISFLOOD is grid-based, and 100 metres grid cells can be employed for medium-sized catchments, but they can be set to 5000 metres for modelling the whole of Europe and up to 0.1° (around 10 km) for modelling globally. LISFLOOD can simulate the long-term water balance (using daily or sub-daily time steps), as well as individual flood events (using hourly or even sub-hourly time intervals).

Although LISFLOOD's primary output product is river discharge, all the internal state variables (soil moisture, for example) can be written as output. All output can be written as maps covering the full computational domain, or time series at user-defined points or areas. The user has complete control on the saving of the output data, thus minimising any waste of disk space or CPU time.

LISFLOOD is implemented in the PCRaster Environmental Modelling Framework (Wesseling et al., 1996), wrapped in a Python-based interface. PCRaster is a raster GIS environment that has its own high-level computer language, which allows for the construction of iterative spatio-temporal environmental models. The Python wrapper of LISFLOOD enables the user to control the model inputs and outputs and the selection of the model modules. This approach combines the power, relative simplicity and maintainability of code written in the PCRaster Environmental Modelling language and the flexibility of Python. LISFLOOD runs on any operating system for which Python and PCRaster are available.

(https://ec-jrc.github.io/lisflood-code/1_introduction_LISFLOOD/)

5.2.1. Model overview

The standard LISFLOOD model setup is made up of the following components:

- a 3-layer soil water balance sub-model;
- sub-models for the simulation of groundwater and subsurface flow (using 2 parallel interconnected linear reservoirs);
- a sub-model for the routing of surface runoff to the nearest river channel;
- a sub-model for the routing of channel flow.

The processes that are simulated by the model include also snow melt, infiltration, interception of rainfall, leaf drainage, evaporation and water uptake by vegetation, surface runoff, preferential flow (bypass of soil layer), exchange of soil moisture between the two soil layers and drainage to the groundwater, sub-surface and groundwater flow, and flow through river channels.



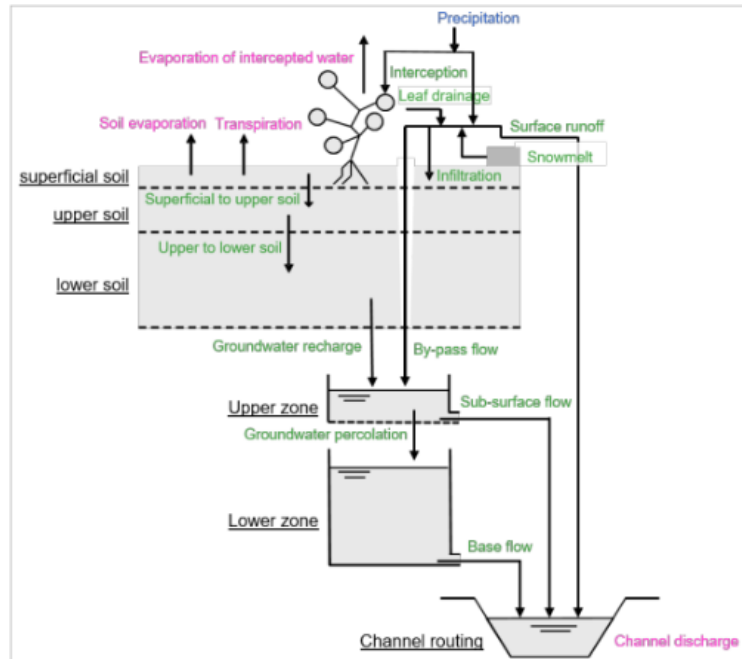


Fig. 5.1. Conceptual model of LISFLOOD

In LISFLOOD a number of parameters are linked directly to land cover classes. In the most recent version of the model, some conceptual changes have been made to render LISFLOOD more land-use sensitive. The spatial distribution and frequency of each land-use class is now defined as a percentage of the whole represented area of the new pixel. The logic behind this approach is that the non-linear nature of the rainfall-runoff processes on different land cover surfaces observed in reality, will be captured better. This concept is also used in models such as SWAT (Arnold and Fohrer, 2005) and PREVAH (Viviroli et al., 2009).

If a part of a pixel is made-up of built-up areas this will influence that pixel's water-balance. LISFLOOD's 'direct runoff fraction's parameter (f_{dr}) defines the fraction of a pixel that is impervious. It's possible to activate any of LISFLOOD's options for writing internal model fluxes to time series or maps.

Standard LISFLOOD processes include:

- Interception
- Evaporation of intercepted water
- Snow melt
- Frost index
- Water available for infiltration and direct runoff
- Water uptake by roots & transpiration
- Evaporation from the soil surface
- Preferential bypass flow
- Infiltration capacity
- Actual infiltration and surface runoff
- Soil moisture redistribution
- Groundwater
- Surface runoff routing
- Sub-surface runoff routing
- Channel routing





- Irrigation
- Water use

While optional simulation processes include:

- Lakes
- Reservoirs
- Polder
- Double kinematic wave
- Dynamic wave
- Soil moisture
- Transmission loss
- Inflow hydrograph
- Water levels
- Variable water fraction
- Transient land use change

Next to the standard outputs of the model, discharge and soil moisture is possible, as well is it possible to activate any specific output including time series of the state variables, report maps of discharge and of water level in rivers etc. (https://ec-jrc.github.io/lisflood-model/3_01_optLISFLOOD_overview/).

5.2.2. Model implementation

LISFLOOD model implementation, as for the SHYFEM model, is described through the description of the case study of Massa (Italy). The mesh defined to run the model is a **100 m** grid covering the Frigido river basin, with 149 x 163 cells.

Frigido is a small river (with a watershed of approximately 63 km², entirely included in the Massa municipality) that originates from the Apuan Alps and has its outlet in Marina di Massa after about 17 km. It has a marked torrential regime with very short response time and, although small, its watershed is quite heterogeneous including the steep slopes and impervious surfaces of the Apuan Alps, the highly urbanized coastal area and complex groundwater mechanisms. It can then be considered a very challenging basin to model. For several aspects, given the overall scope of the SCORE project, simplified approaches will be used.

As described in detail in the step by step model user guide (<https://ec-jrc.github.io/lisflood-code/>) the following steps are needed for the model implementation:

- preparing the settings file;
- preparing the input files;
- initialization of the model;
- calibration (model run for selected past events and comparison with available river discharge and water level observations);
- running.

The final model-run will be performed for the whole time span of EUROCORDEX (2006-2100) data for the selected climatological scenarios, with a time step of 3 hours.



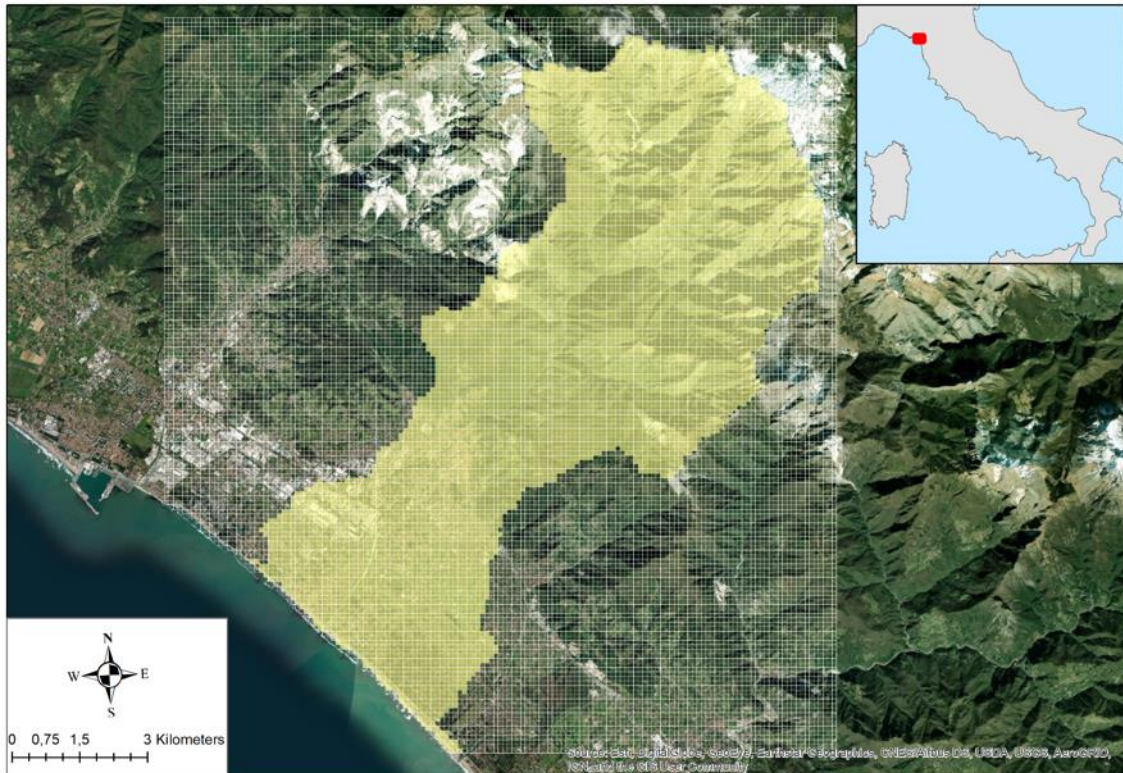


Fig.5.2. LISFLOOD model grid and Basin mask for Frigido river (two small coastal catchments are also included).

5.2.3. Settings file

The settings file is an *xml* file containing the process-related parameters. These are all defined in the '*lfuser*' element, and default values are given for each of them. In the description of these parameters the guide provides some suggestions as to which parameters should be used for calibration, and which ones are better left untouched.

On Github there is also a repository which contains the datasets of two different use cases to test the model (<https://github.com/ec-jrc/lisflood-code/tree/master/tests/data>).

The following steps have been accomplished:

- 1) specify the file path;
- 2) define time-related specifications;
- 3) add parameter options;
- 4) choose the optional model routines (defining which ones are available; what they do; and how to "activate" them).

At a first run it is highly recommended to run the model with the basic options. In the present implementation the first tests were conducted with the *base.xml* settings file (https://github.com/ec-jrc/lisflood-code/blob/master/tests/data/LF_ETRS89_UseCase/settings/base.xml)





5.2.4. Input datasets

- Meteorological forcing

Atmospheric variables (precipitation, air temperature and humidity, radiation, windspeed) data provided by CORDEX project (EUROCORDEX domain) were used as model forcing data. EUROCORDEX data have a 0.11 degrees spatial resolution and 3-hourly temporal resolution. These datasets have been converted into single day files of 8 temporal steps and re-gridded from native Lambert Conical projection to the Lambert equal area projection (EPSG:3035; the projection used for all the input layers), in a grid of 12 km spatial resolution.

Since the study area (covering the Frigido river basin) is quite small, only 4 cells of the forcing layers overlap the model grid. Clearly, for hydrological simulations in such small watersheds, appropriate downscaling of atmospheric forcing data (at least rainfall fields) is advisable. However, since finer scale rainfall fields are not available yet (they might be provided in the future with the methodology described in Section 2), the original EUROCORDEX data were resampled at model resolution (100 m) with the simple nearest-neighbour interpolation. This dataset may be considered the best choice in terms of availability and homogeneity and, whilst undoubtedly too coarse for a very small basin like Frigido, might be suitable for the watersheds of the other coastal cities in the SCORE project.

- Static maps

All the static maps were derived with 100 m spatial resolution, according to the resolution of the model grid. All the static maps are produced as netCDF files (.nc).

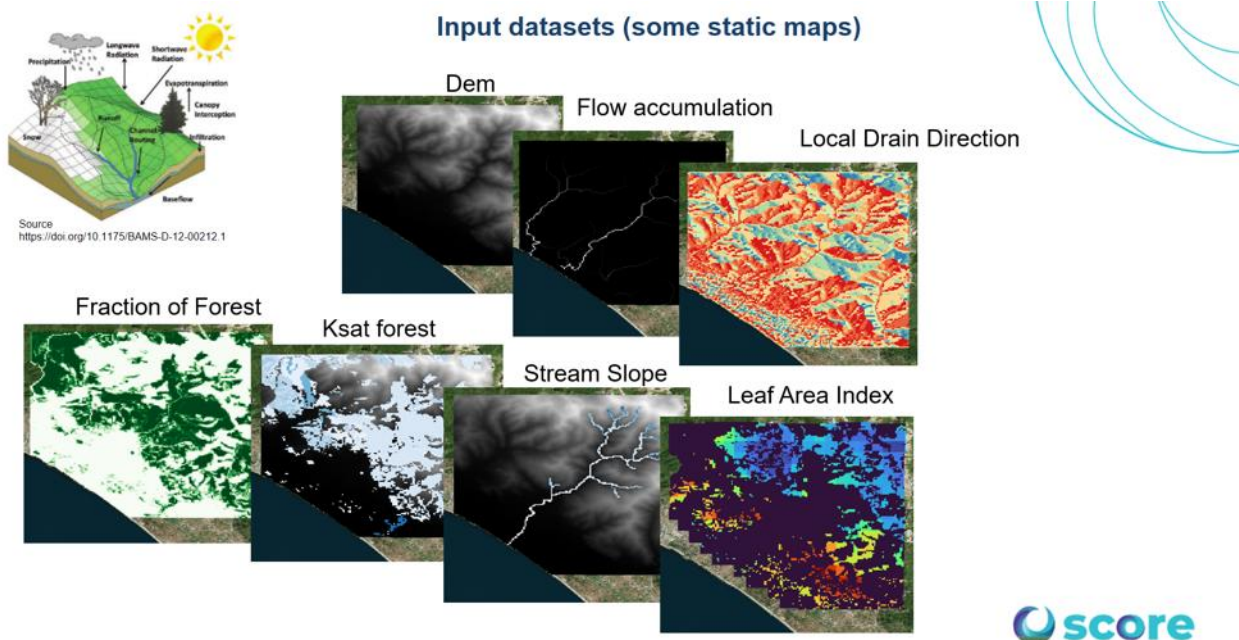


Fig.5.3. Some examples of LISFLOOD model input static layers plotted in QGIS.





Topography

Topography maps are derived from the digital elevation model (DEM). In this implementation the DEM derived from the generalization of the 10 m spatial resolution DEM from Tuscany Regional Administration in QGIS, as all the other Topography layers.

The Local Drain Direction is the essential component to connect the grid cells to express the flow direction from one cell to another and forming a river network from springs to mouth; the Upstream area (or flow accumulation) is the accumulated area of all connected water pixels that in a river network starts at the springs and goes to the river mouth; both these layers were obtained using the PC Raster plugin. The Gradient and the Standard elevation layers are used for snow processes and for routing of surface runoff. They were obtained using the slope tool and the raster calculator.

Land Use maps

The LISFLOOD hydrological model can distinguish the following land cover types: forest, inland water, sealed surface (impervious urban area), irrigated land, rice, and other land cover type. Interception, evapotranspiration, infiltration, and overland (or surface) flow respond differently to each surface type.

Fraction of inland water map

Inland water map includes information on rivers, freshwater and saline lakes, ponds and other permanent water bodies on the continents. In the LISFLOOD model the inland water fraction map is used to identify the fraction of the pixel covered by open water bodies, where the most prominent hydrological process is evaporation. Since no inland water bodies were present in the area, this layer was not computed, and only a check of consistency between coastal water fractions and computational area masking was performed.

All the following layers were computed in QGIS as a generalization (essentially aggregation, amalgamation and merge; see <http://52north.github.io/wps-profileregistry/concept/generalization.html>) from the 10 m resolution regional land use dataset.

Fraction of sealed surface map

Here, the sealed surface map describes urban areas, characterizing the human impact on the environment.

Fraction of forest map

Forest map describes land use composed of evergreen and deciduous needle leaf and broad leaf trees.

Fraction of irrigated crops map

Irrigated crops map includes all possible crops excluding rice (that is modelled separately).

Fraction of other land cover type map

Other land cover type map includes agricultural areas, non-forested natural area, pervious surface of urban areas.

Land Use depending maps

Every land use is characterised by a series of coefficients, such as the crop coefficient, the crop group number, the Manning's surface roughness coefficient and the soil depths. Starting from the land use maps previously obtained, each of these for the respective land cover are derived from the appropriate literature, and then aggregated into three maps, one for forested areas (evergreen and deciduous needle leaf and broadleaf trees), one for irrigated crops (excluding rice), and one for the other land cover type areas, such as agricultural areas, non-forested natural area, pervious surface of urban areas.





- Crop Coefficient: is defined as the ratio between the potential evapotranspiration rate, in mm/day, and the potential evaporation rate of a specific crop. Crop coefficients of each land cover class are obtained from Nistor, 2018 [11].
- Crop number: represents a vegetation type and is an indicator of its adaptation to dry climate. In LISFLOOD it is used in the computation of the critical amount of soil moisture below which water uptake from plants is reduced as they start closing their stomata. Crop numbers of each land cover class, as well as the Manning's coefficients, are obtained from Burek et al., 2014 [6].
- Manning's surface roughness coefficient: represents the friction applied to the flow by the surface on which water is flowing. In LISFLOOD it is used to compute surface runoff routing for each land use category.
- Soil depth layers 1, 2 and 3: used to compute the available water storage volume in the soil. In LISFLOOD three soil layers are used to model the hydrological processes in the soils. The layers take into account forest and non-forest root depths to divide the total soil depth between hydrological processes of the topsoil (surface layer or layer 1, and middle layer or layer 2) and subsoil (bottom layer or layer 3).

The methodology for calculating the depth of the 3 soil layers was adapted from Burek et al., 2014 [6]. The total soil depth is considered as the "absolute depth to bedrock" and the "rooting depth" for forest, and non-forest fractions are calculated according to the above methodology. Soil depth is expressed in mm.

Soil horizon depth strata were derived from the soil database, created by soil profiles and soil wells, available for a near basin (Carrione river).

For each dominant soil type in the map units of the soil map, average thicknesses of soil horizons were calculated following the methodology given for the model, based on soil depth (absolute soil depth) and useful depth to roots (rooting depth), with the depth understood as measured from ground level, to which tree plant roots can extend.

Layer 1 soil depth (surface) for forest and non-forest areas ($SD1$) is assumed constant, equal to 50 mm:

$$(1) SD1=50 \text{ mm}$$

Soil depth layers 2 (middle, $SD2$) and 3 (lower, $SD3$) for forest/non-forest are calculated in several steps: first at the native resolution of the input data set, then at the required resolution.

For soil depth layer 2 (middle, $SD2$), if the absolute soil depth is ≤ 300 mm, then (2) $SD2 = (\text{absolute depth} - SD1)/2$

If >300 mm, then

$$(3) SD2 = \min(\text{root depth}, (\text{absolute depth} - 300 \text{ mm} - SD1))$$

If the calculated value of $SD2$ is less than 50 mm, $SD2 = 50$ mm is used.

For soil depth layer 3 (bottom layer, $SD3$).

$$(4) SD3 = \text{absolute depth} - (SD1 + SD2)$$

Surfaces with outcropping rock and non-soil surfaces (roads, urban, quarries) were given 'No Data' values, except for surfaces with significant man-made quarry deposits (ravines), which were given an absolute depth of 150 cm and hydrological parameters of sandy soils.





Soil hydraulic properties

Soil hydraulic parameters are used to calculate water dynamics through a vertical soil profile.

In the LISFLOOD model the relationship between soil moisture and suction pressure (water retention curve), and hydraulic conductivity and soil moisture is described by the Van Genuchten equation and requires the following parameters: saturated hydraulic conductivity, *lambda*, *genu alpha*, *theta* residual and *theta* saturated.

- *Theta saturated* (θ_{s}) is the saturated water content soil hydraulic property representing the maximum water content in the soil;
- *Theta residual* (θ_{r}) is the residual water content soil hydraulic property representing the minimum water content in the soil;
- *Lambda* is the Van Genuchten parameter λ (also referred as 'n-1' in literature) soil hydraulic property representing the pore size index of the soil;
- *Genu alpha* (*genua*) is the Van Genuchten parameter α soil hydraulic property;
- *K saturated* (K_{sat}) is the saturated hydraulic conductivity soil hydraulic property describing the ease with which water moves through pore-spaces of the soil.

Moreover, LISFLOOD differentiates between the water dynamics of areas with topsoil covered by forest and topsoil covered by non-forest land types. Here, forest includes evergreen and deciduous needle leaf and broad leaf trees, and non-forest (also referred to as 'others') includes all the other land cover types apart from forest.

The hydrological parameters for each soil horizon, estimated Water Retention and Saturated Hydraulic Conductivity, were calculated by pedofunctions (Brackensiek, 1984; Wosten, 1998) from measured data of grain size, organic carbon and bulk density. The parameters obtained for each soil horizon were then transferred to the depths defined in LISFLOOD model (*SD1*, *SD2*, *SD3*).

Channel geometry

In the LISFLOOD model, flow through the channel is simulated using the kinematic wave equations. Channel maps describe the sub-grid information of the channel geometry, i.e. the length, slope, width and depth of the main channel inside a grid-cell. All these parameters have been computed in *R*.

In the present implementation, the channel mask map, used to identify the cells that have channels, was computed from a rasterization of the vector dataset of the rivers from the regional database. The channel side slope map was computed by dividing the horizontal distance by vertical distance of the side slope of the channels; here '1' was assigned to all the grid cells, which correspond to a 45° angle of the side slope (and it is the default value used in our implementation). The channel length is a parameter used to take into account the river meandering paths. It can be easily computed in a GIS environment or in *R*. In the present implementation, no meanderings being present, a unique value = 1 (as an *nc*-file with constant values) has been used. The channel gradient map is the gradient along the channel cells. It was computed using the *whitebox* package (implementation of *WhiteboxTools* in *R* stats <https://cran.r-project.org/web/packages/whitebox/vignettes/demo.html>). The Manning's roughness coefficient for channels can be derived from literature or previous studies.





The channel bottom width (*chanbw*) map was computed using empirical relationship that relate channel width of the grid-cell with its upstream area (in km²); for example, following Burek et al. (2014):

$$chanbw=0.0032 \cdot upstreamArea$$

The floodplain width (in m) was computed using the following equation from Burek et al. (2014):

$$floodplainWidth=3 \cdot chanbw$$

The channel bankfull depth can be computed in two steps. The first step uses the empirical relationship relating the channel bankfull depth of the grid-cell with its upstream area (in km²) following Burek et al. (2014):

$$chanbnkfstep_1=0.27 \cdot upstreamArea^{0.33}$$

The second step uses Manning's equation following Burek et al. (2014). The LISFLOOD model first needs to be run for the calibration period length with the initial channel bottom width and bankfull depth parameters to get a long-term average discharge (*avgdis*) which is then used in the Manning's equation:

$$chanbnkfstep_2=1.004 \cdot chanman^{0.6} \cdot (2 \cdot avgdis)^{0.6} \cdot chanbw^{-0.6} \cdot changrad^{-0.3}$$

Leaf area index

The Leaf Area Index (LAI) is a dimensionless parameter defined as the one-sided green leaf area per unit ground surface area, therefore quantifies the thickness of the vegetation cover. Also, for this index separated maps for forested areas, irrigated crops and other land uses are requested, and for each of these, 10-day average maps must be prepared (e.g. a map describing the LAI values of the decade 1-10 January, another one for the period 11-20 January, and so on). In order to obtain these inputs the Copernicus Global Land Service LAI Collection Version 2 has been used (<https://land.copernicus.eu/global/products/lai>). It provides LAI data from November 1998 to June 2020 merged in decade averages, just as the LISFLOOD model needs. The data processing consists in calculating the average of the data of all the available years, for all the 36 decades of a year, in order to obtain the 36 maps. Later, for each of these, separated maps regarding only forested areas (36 "*laif*"), irrigated crops ("*laii*") and other land uses (36 "*laio*") are extracted. To be precise, fraction maps of the cover type in questions are used to mask LAI maps, setting at zero value the areas with a covering percentage of the land use itself less than 70%.

(https://ec-jrc.github.io/lisflood-code/4_Static-Maps_leaf-area-index/)

Other data

Reservoirs and lakes, rice calendar, inflow points and water demand maps were not computed because of their absence in the area. So the relative sub-routines were not activated in the setting file.

Outlet points: locations and *IDs* of the points for which LISFLOOD provides the time series of discharge values. The number of such points can be arbitrary (depending of the points of interest). In our case, one point is placed in order to be used as an upstream boundary condition for the 2D hydraulic flood model, other output





points are in correspondence to existing hydrometric gauges (for calibration and validation). Other points, like specific geographical points of interest in the study area can be added.

5.2.5. Outputs

The model predictions in terms of river discharge (time series of discharge at given points in the river network) as well as other state variables that can be relevant (e.g., soil moisture), obtained from the application of the model for specific climatic scenarios (not described in this report), will be processed in order to define the reference events and their probability of occurrence.

More specifically, the 3-hourly time series of discharges for the period 2006-2100 at selected given points in the Frigido streamline in the proximity of the outlet will be analysed with specific statistical tools developed also in Task 3.3 that will allow to reconstruct the peak discharges and hydrographs with selected return periods in a climate change scenario.

Such events will be adopted as input data for the high-resolution Hydraulic model (not described in this report) to compute the effects of the peak discharge on the inundation of the near shore zones.





6. CONCLUSIONS AND RECOMMENDATION

The present document describes the methodology and the numerical tools employed for the downscaling of climate data, from a synoptic scale, to a spatial scale which allows us to model urban floods in coastal cities due to the interplay of wave patterns and properties, storm surges and river discharges.

This means we provide the information and the steps to create datasets and time series of wave patterns, sea water level and rainfall rate at specific locations corresponding to the CCLLs. These datasets can be used to analyse the effects, that modifications induced by climate change on the atmospheric circulation have, on the flood events at the local scale.

Climate data come from the EUROCORDEX project. More specifically, the ALADIN 63 RCM that provides the input variables for the downscaling procedure. This RCM is used within the EUROCORDEX project to downscale information from GCMs, using initial and boundary condition data from the ERA-INTERIM reanalysis (evaluation run) and from the CNRM-CM5 model (historical, RCP4.5 and RCP8.5 runs).

Data from evaluation and historical runs are used to assess the reliability of the downscaling procedure we proposed, whereas the rcp4.5 and rcp8.5 runs are used to evaluate the impact of climate change on the flood events at the CCLLs.

Sea water levels are downscaled through the 2D, barotropic version of the SHYFEM model forced by winds and atmospheric pressure. The simulations are modulated with the sea level rise signal.

Wave climate is produced by the WWIII spectral wave model forced by surface winds.

Both the sea level and the wave model are implemented on unstructured grids to ensure a high spatial resolution at the coastal locations analysed.

River discharges are obtained by the hydrological model implemented on the river basins associated with the analysed coastal city. The rainfall rate to feed the hydrological model is downscaled from the RCM through a statistical downscaling tool based on neural networks.

The method has been designed and tested for the statistical spatial downscaling of the atmospheric projection data from the CORDEX databases. Spatial downscaling can in fact be necessary in some applications, such as hydrological projections for small hydrological basins. The method makes use of a NN approach (namely a CNN approach). The training is based on matching two tool datasets, one at the projection (coarser) resolution, the other at the target (finer) resolution. The former is generated upscaling the latter, to guarantee a perfect temporal and spatial coherence between data. The latter has to be available from past runs for a climatological significant period. A further step is needed to match statistical distributions between the tool coarser resolution data and the projection data for a historical period climatologically consistent with the tool data one. For this step we propose the probability matching method. The whole process is not to be considered a plug-and-play solution, because of the complexities of the data and the related processes under analyses. Hence, several things, especially in the NN steps, would need specific tuning when applied to specific datasets. However it does not change the proposed processing





scheme and the basic tools that were developed. In addition to spatial downscaling, the developed tools can also address the problem of the local downscaling, i.e. the transformation of the projection data into equivalent projection measurements from a local station, located in the target coastal cities.

The dataset produced following this methodology will be used to perform an extreme value analysis (EVA) with variable time parameters to identify synthetic events to simulate urban flood at different time in the future and for different emission scenarios (RCP4.5 and RCP8.5 runs).





7. REFERENCES

- [1] Alberola, C., Rousseau, S., Millot, C., Astraldi, M., Font, J., Lafuente, J., Gasparini, G.-P., Send, U., & Vangriesheim, A. (1995). Tidal currents in the Western Mediterranean Sea. *Oceanologica Acta*, 18, 273–284.
- [2] Barbariol, F., Davison, S., Falcieri, F. M., Ferretti, R., Ricchi, A., Sclavo, M., & Benetazzo, A. (2021). Wind Waves in the Mediterranean Sea: An ERA5 Reanalysis Wind-Based Climatology. *Frontiers in Marine Science*, 8. <https://doi.org/10.3389/fmars.2021.760614>
- [3] Benestad, R. (2016). Downscaling climate information. In *Oxford research encyclopedia of climate science*.
- [4] Bonaduce, A., Staneva, J., Grayek, S. et al. Sea-state contributions to sea-level variability in the European Seas. *Ocean Dynamics* 70, 1547–1569 (2020). <https://doi.org/10.1007/s10236-020-01404-1>
- [5] Brakensiek, D.L. Rawls, W.J. Stephenson, G.R. (1984). Modifying SCS hydrologic soil groups and curve numbers for rangeland soils ASAE Paper No. PNR-84-203.
- [6] Burek P., Bianchi A., Gentile A. (2014). A Pan-European Data Set for hydrological modelling. JRC Technical Reports. https://ec-jrc.github.io/lisflood/pdfs/Dataset_hydro.pdf
- [7] Capecchi, V., Pasi, F., Gozzini, B., Brandini, C. A convection-permitting and limited-area model hindcast driven by ERA5 data: precipitation performances in Italy, 29 August 2022, PREPRINT (Version 1) available at Research Square [<https://doi.org/10.21203/rs.3.rs-1978157/v1>]
- [8] Coles, S., Bawa, J., Trenner, L., & Dorazio, P. (2001). An introduction to statistical modeling of extreme values (Vol. 208, p. 208). London: Springer.
- [9] Coppola E., Nogherotto R., Ciarlò J.M., Giorgi F., van Meijgaard E., Kadygrov N., Iles C., Corre L., Sandstad M., Somot S., Nabat P., Vautard R., Levavasseur G., Schwingshackl C., Sillmann J., Kjellström E., Nikulin G., Aalbers E., Lenderink G., Christensen O.B., Boberg F., Lund Sørland S., Demory M.-E., Bülow K., Teichmann C., Warrach-Sagi K., Wulfmeyer V. (2021) Assessment of the European Climate Projections as Simulated by the Large EURO-CORDEX Regional and Global Climate Model Ensemble. *Journal of Geophysical Research – Atmospheres*, 2021, vol. 126, no 4, <http://doi.org/10.1029/2019JD032356>.
- [10] Danilov, S. (2013). Ocean modeling on unstructured meshes. *Ocean Modelling*, 69, 195–210. <https://doi.org/https://doi.org/10.1016/j.ocemod.2013.05.005>
- [11] Dee, D. P., Uppala, S. M., Simmons, A. J., Berrisford, P., Poli, P., Kobayashi, S., ... & Vitart, F. (2011). The ERA-Interim reanalysis: Configuration and performance of the data assimilation system. *Quarterly Journal of the royal meteorological society*, 137(656), 553-597.
- [12] European Union, Copernicus Land Monitoring Service 2018, European Environment Agency (EEA).
- [13] Fagundes, M., Litvin, S.Y., Micheli, F. et al. Downscaling global ocean climate models improves estimates of exposure regimes in coastal environments. *Sci Rep* 10, 14227 (2020). <https://doi.org/10.1038/s41598-020-71169-6>
- [14] Ferrarin, C., Davolio, S., Bellafiore, D., Ghezzi, M., Maicu, F., Kiver, W. M., Drofa, O., Umgieser, G., Bajo, M., Pascalis, F. De, Malguzzi, P., Zaggia, L., Lorenzetti, G., & Manfè, G. (2019). Cross-scale operational oceanography in the Adriatic Sea. *Journal of Operational Oceanography*, 12(2), 86–103. <https://doi.org/10.1080/1755876X.2019.1576275>





- [15] Jacob, D., Petersen, J., Eggert, B., Alias, A., Christensen, O. B., Bouwer, L. M., ... & Yiou, P. (2014). EURO-CORDEX: new high-resolution climate change projections for European impact research. *Regional environmental change*, 14(2), 563-578.
- [16] Jacob, D., Teichmann, C., Sobolowski, S., Katragkou, E., Anders, I., Belda, M., Benestad, R., Boberg, F., Buonomo, E., Cardoso, R. M., & others. (2020). Regional climate downscaling over Europe: perspectives from the EURO-CORDEX community. *Regional Environmental Change*, 20(2), 1–20.
- [17] Kamidaira, Y., Kawamura, H., Kobayashi, T., Uchiyama, Y., (2019) Development of regional downscaling capability in STEAMER ocean prediction system based on multi-nested ROMS model, *Journal of Nuclear Science and Technology*, 56:8, 752-763, DOI: 10.1080/00223131.2019.1613269
- [18] IPCC 2013. Climate change 2013: the physical science basis: Working Group I contribution to the Fifth assessment report of the Intergovernmental Panel on Climate Change. (Stocker, T. Ed.) Cambridge university press.
- [19] Lionello, P., Barriopedro, D., Ferrarin, C., Nicholls, R. J., Orlić, M., Raichich, F., Reale, M., Umgiesser, G., Vousdoukas, M., and Zanchettin, D.: Extreme floods of Venice: characteristics, dynamics, past and future evolution (review article), *Nat. Hazards Earth Syst. Sci.*, 21, 2705–2731, <https://doi.org/10.5194/nhess-21-2705-2021>
- [20] Liu, ZJ., Minobe, S., Sasaki, Y.N. et al. Dynamical downscaling of future sea level change in the western North Pacific using ROMS. *J Oceanogr* 72, 905–922 (2016). <https://doi.org/10.1007/s10872-016-0390-0>
- [21] Nistor, M. (2018). Projection of Annual Crop Coefficients in Italy Based on Climate Models and Land Cover Data. *Geographia Technica*.
- [22] Pawlowicz, R., Beardsley, B., & Lentz, S. (2002). Classical tidal harmonic analysis including error estimates in MATLAB using T_TIDE. *Computers & Geosciences*, 28(8), 929–937. [https://doi.org/https://doi.org/10.1016/S0098-3004\(02\)00013-4](https://doi.org/https://doi.org/10.1016/S0098-3004(02)00013-4)
- [23] Pham, V. S., Hwang, J. H., & Ku, H. (2016). Optimizing dynamic downscaling in one-way nesting using a regional ocean model. *Ocean Modelling*, 106, 104–120. <https://doi.org/https://doi.org/10.1016/j.ocemod.2016.09.009>
- [24] Quattrocchi, G., Simeone, S., Pes, A., Sorgente, R., Ribotti, A., & Cucco, A. (2021). An operational numerical system for oil stranding risk assessment in a high-density vessel traffic area. *Frontiers in Marine Science*, 8, 133.
- [25] Rockel, B. The Regional Downscaling Approach: a Brief History and Recent Advances. *Curr Clim Change Rep* 1, 22–29 (2015). <https://doi.org/10.1007/s40641-014-0001-3>.
- [26] Rosenfeld, D., Wolff, D.B., Atlas, D., 1993. General Probability-matched Relations between Radar Reflectivity and Rain Rate. *Journal of Applied Meteorology and Climatology*. [https://doi.org/10.1175/1520-0450\(1993\)032<0050:GPMRBR>2.0.CO;2](https://doi.org/10.1175/1520-0450(1993)032<0050:GPMRBR>2.0.CO;2)
- [27] Ruti, P. M., Somot, S., Giorgi, F., Dubois, C., Flaounas, E., Obermann, A., Dell’Aquila, A., Pisacane, G., Harzallah, A., Lombardi, E., Ahrens, B., Akhtar, N., Alias, A., Arsouze, T., Aznar, R., Bastin, S., Bartholy, J., Béranger, K., Beuvier, J., Bouffies-Cloch e, S., Brauch, J., Cabos, W., Calmanti, S., Calvet, J.-C., Carillo, A., Conte, D., Coppola, E., Djurdjevic, V., Drobinski, P., Elizalde-Arellano, A., Gaertner, M., Gal n, P., Gallardo, C., Gualdi, S., Goncalves, M., Jorba, O., Jord , G., L’Heveder, B., Lebeaupin-Brossier, C., Li, L., Liguori, G., Lionello, P., Maci s, D., Nabat, P.,  nol, B., Raikovic, B., Ramage, K., Sevault, F., Sannino, G., Struglia, M. V., Sanna, A., Torma, C., & Vervatis, V. (2016). Med-CORDEX Initiative for Mediterranean Climate Studies, *Bulletin of the American Meteorological Society*, 97(7), [1187-1208](https://doi.org/10.1175/1520-0450(1993)032<0050:GPMRBR>2.0.CO;2).





- Retrieved Dec 12, 2022, from <https://journals.ametsoc.org/view/journals/bams/97/7/bams-d-14-00176.1.xml>
- [28] Sannino, G., Carillo, A., Iacono, R., Napolitano, E., Palma, M., Pisacane, G., & Struglia, M. (2022). Modelling present and future climate in the Mediterranean Sea: a focus on sea-level change. *Climate Dynamics*, 1-35.
- [29] Smagorinsky, J. (1993). Some historical remarks on the use of non-linear viscosities, in *Large Eddy Simulation of Complex Engineering and Geophysical Flows*, edited by B. Galperin and S. A. Orszag, pp. 3–36, Cambridge Univ. Press, Cambridge, U. K.
- [30] Taylor, K. E., Stouffer, R. J., & Meehl, G. A. (2012). An overview of CMIP5 and the experiment design. *Bulletin of the American meteorological Society*, 93(4), 485-498.
- [31] Trotta, F., Pinardi, N., Fenu, E. et al. Multi-nest high-resolution model of submesoscale circulation features in the Gulf of Taranto. *Ocean Dynamics* 67, 1609–1625 (2017). <https://doi.org/10.1007/s10236-017-1110-z>
- [32] Umgiesser, G., Canu, D. M., Cucco, A., & Solidoro, C. (2004). A finite element model for the Venice Lagoon. Development, set up, calibration and validation. *Journal of Marine Systems*, 51(1–4), 123–145. <https://doi.org/10.1016/j.jmarsys.2004.05.009>
- [33] Umgiesser, G., Ferrarin, C., Bajo, M., Bellafiore, D., Cucco, A., De Pascalis, F., Ghezzi, M., McKiver, W., & Arpaia, L. (2022). Hydrodynamic modelling in marginal and coastal seas — The case of the Adriatic Sea as a permanent laboratory for numerical approach. *Ocean Modelling*, 179, 102123. <https://doi.org/https://doi.org/10.1016/j.ocemod.2022.102123>
- [34] Zampato, L., Umgiesser, G., & Zecchetto, S. (2006). Storm surge in the Adriatic Sea: Observational and numerical diagnosis of an extreme event. *Advances in Geosciences*, 7, 371 – 378. <https://doi.org/10.5194/adgeo-7-371-2006>
- [35] Zheng, L., & Weisberg, R. H. (2012). Modeling the west Florida coastal ocean by downscaling from the deep ocean, across the continental shelf and into the estuaries. *Ocean Modelling*, 48, 10–29. <https://doi.org/https://doi.org/10.1016/j.ocemod.2012.02.002>
- [36] The Copernicus Climate Change Service (C3S) [Internet]. Available from: <https://climate.copernicus.eu/about-us>
- [37] SCORE D5.2 Data Management Plan Document [Internet]. Available from: <https://mailitsligo.sharepoint.com/sites/SCORE-H2020/Shared%20Documents/Forms/AllItems.aspx?id=/sites/SCORE-H2020/Shared%20Documents/WP5/Deliverables/D5.2/SCORE-deliverable-D5.2-V1.1.pdf&parent=/sites/SCORE-H2020/Shared%20Documents/WP5/Deliverables/D5.2>
- [38] SCORE D11.1-Ethics requirement: Standard Ethical Protocol [Internet]. Available from: <https://mailitsligo.sharepoint.com/sites/SCORE-H2020/Shared%20Documents/Forms/AllItems.aspx?id=%2Fsites%2FSCORE%2DH2020%2FShared%20Documents%2FWP11%2FSCORE%2Ddeliverable%2DD11%2E1%2DMSG%2DFinal%2Epdf&parent=%2Fsites%2FSCORE%2DH2020%2FShared%20Documents%2FWP11>
- [39] Vannucchi, V., Taddei, S., Capecchi, V., Bondoni, M., Brandini, C. (2021). Dynamical Downscaling of ERA5 Data on the North-Western Mediterranean Sea: From Atmosphere to High-Resolution Coastal Wave Climate. *J. Mar. Sci. Eng.*, 9, 208-235. <https://doi.org/10.3390/jmse9020208>.
- [40] Vautard R., Kadyrov N., Iles C., Boberg F., Buonomo E., Bülow K., Coppola E., Corre L., van Meijgaard E., Nogherotto R., Sandstad M., Schwingshackl C., Somot S., Aalbers E., Christensen O.B., Ciarlo J.M., Demory M.-E., Giorgi F., Jacob D., Jones R.G., Keuler K., Kjellström E., Lenderink G., Levvasseur G., Nikulin G., Sillmann J., Solidoro C., Lund Sørland S., Steger C., Teichmann C., Warrach-Sagi K.,





- Wulfmeyer V. (2021) Evaluation of the large EURO-CORDEX regional climate model ensemble. *Journal of Geophysical Research – Atmospheres*, <https://doi.org/10.1029/2019JD032344>, <http://dx.doi.org/10.1029/2019JD032344>
- [41]Voldoire A, Sanchez-Gomez E, y Méliá DS, Decharme B, Cassou C, Sénési S et al (2013) The CNRM-CM5. 1 global climate model: description and basic evaluation. *Clim Dyn* 40(9–10):2091–2121.
- [42]Vousdoukas, M. I., Voukouvalas, E., Annunziato, A., Giardino, A., & Feyen, L. (2016). Projections of extreme storm surge levels along Europe. *Climate Dynamics*, 47(9), 3171-3190.
- [43] Wösten J.H.M., Lilly A., Nemes A., Le Bas C. (1998). Using existing soil data to derive hydraulic parameters for simulation models in environmental studies and in land use planning, Final Rep. Eur. Un., Wageningen.
- [44]WAVEWATCH III Development Group, 2016: User manual and system documentation of WAVEWATCH III version 5.16. NOAA / NWS / NCEP / MMAB Technical Note 329, 326 pp. + Appendices.

